Contents lists available at ScienceDirect

Engineering

journal homepage: www.elsevier.com/locate/eng

Research
Tissue Engineering—Review

细胞行为在基质刚性和纳米拓扑结构上的生物物理调控

Yong Yang [a,*], Kai Wang [a], 顾晓松 [b], Kam W. Leong [c,*]

[a] Department of Chemical and Biomedical Engineering, West Virginia University, Morgantown, WV 26506, USA
[b] Key Laboratory of Neuroregeneration of Jiangsu and the Ministry of Education, Co-Innovation Center of Neuroregeneration, Nantong University, Nantong, Jiangsu 226001, China
[c] Department of Biomedical Engineering, Columbia University, New York, NY 10027, USA

ARTICLE INFO

Article history:
Received 11 January 2017
Revised 24 January 2017
Accepted 25 January 2017
Available online 21 February 2017

关键词
细胞外基质
刚性
纳米拓扑结构
黏附配体
细胞行为

摘要

细胞外基质 (ECM) 的刚性和纳米拓扑结构影响生物体发育及生理和病理进程。因此，这些生物物理特征被用于调节细胞黏附、铺展至增殖、分化的各种细胞行为。描述细胞行为的生物物理调节对合理设计新型生物材料、植入物和医疗装置十分关键。已有学者就基质刚性和纳米拓扑结构特征对细胞行为的影响分别进行了综述，然而，刚性和纳米拓扑结构与细胞行为的交织影响尚未有人总结。此次，我们首次综述了基质刚性和纳米拓扑结构对细胞行为的影响，然后聚焦于生物物理信号从整合素到细胞核的细胞内传递，并试图将细胞行为的细胞外调节与基质的生物物理学特征联系在一起。最后，我们讨论了在剖析细胞行为的生物物理调节和将基质的刚性和纳米拓扑结构生物力学特性转化到组织工程和再生医学时存在的挑战。

1. 引言

越来越多的研究表明，细胞命运受细胞外基质(ECM)的刚性和纳米拓扑结构特征影响。ECM由包括胶原蛋白、弹性蛋白和纤连蛋白在内的多种纳米尺寸的生物大分子构成[1]，通常表现为纳米尺度的拓扑结构，如图1(a) [2–8]所示。例如，直径为几微米的胶原纤维由直径为10~300 nm的胶原原纤维分级构成[9,10]。肺间质基质表现为纳米级纤维胶原蛋白与弹性蛋白的交联框架[8,11]。根据ECM的组成以及间质液的不同[12]，ECM表现出不同刚性，如图1(b) [13–15]所示。基质的生物物理学(刚性和纳米拓扑结构)特征与影响其时空排列的生物化学和生物力学特征一起调节细胞表型和功能。

ECM的刚性和纳米拓扑结构影响生物体发育及生理和病理进程[16–20]。例如，疾病状态可以改变组织刚性。乳腺组织的刚性可从正常状态下的约1 kPa增加到乳腺癌时的约4 kPa [21]。与正常状态下相比，肺刚性在肺气肿时降低[22]，但在纤维化组织中则升高[23,24]。此外，成纤维细胞会对由细胞增殖和胶原蛋白合成引起的基质刚性增加产生反应；诱导的ECM硬化可以进一步通过正反馈回路促进、扩大和维持纤维化[24,25]。

基质的生物物理学特征已被用于调节细胞行为的各个方面[26]。自从1997年的第一次报道出现后[27]，已有许多证据表明基质刚性在调节细胞行为和许多生物进

* Corresponding authors.
E-mail addresses: yong.yang@mail.wvu.edu; kam.leong@columbia.edu

2095-8099/
英文原文: Engineering 2017, 3(1): 36–54
引用本文: Yong Yang, Kai Wang, Xiaosong Gu, Kam W. Leong. Biophysical Regulation of Cell Behavior—Cross Talk between Substrate Stiffness and Nanotopography. *Engineering*, http://dx.doi.org/10.1016/J.ENG.2017.01.014

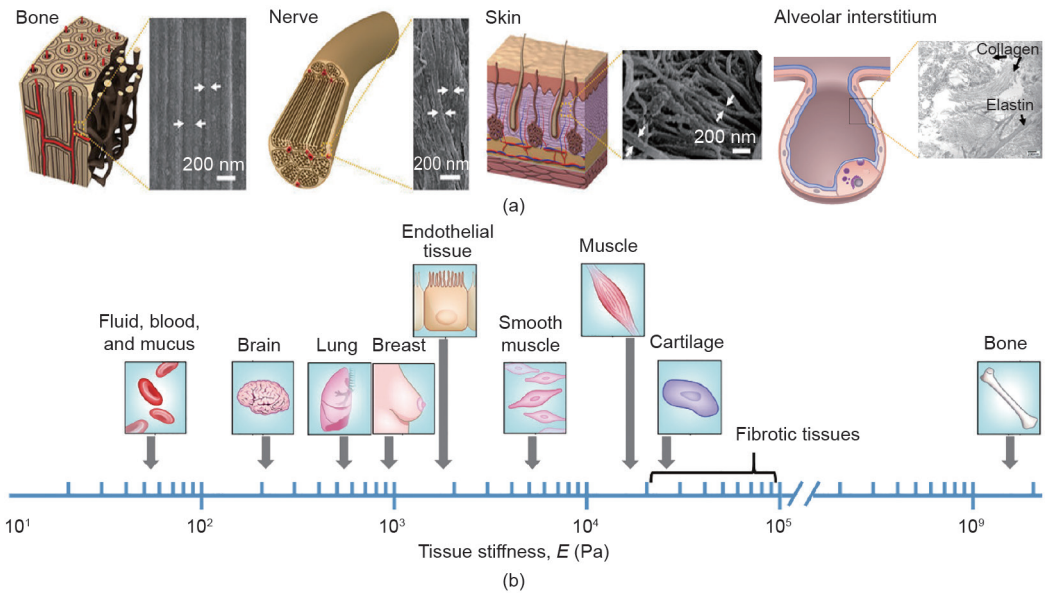

图1. 人体组织的生物物理学特性。(a)各种组织中的纳米结构示意图。箭头所指为各种纳米结构。骨骼、神经和皮肤的示意图和扫描电子显微镜(SEM)图像授权改编自参考文献[6]。肺泡间质的示意图和SEM图像分别改编自参考文献[7]和[8]。(b)人体组织刚性示意图。与正常状态下的组织刚性相比，纤维化组织的刚性较大。授权改编自参考文献[15]。

程中发挥重要作用[27–32]。例如，C2C12小鼠成肌细胞只在具有正常肌肉典型刚性的聚丙烯酰胺(PAAm)凝胶上显示出明确的肌动球蛋白条纹，而在更软的(刚性较低的)凝胶或更硬的玻璃基质上则不会表现出上述特征[33]。此外，与脑、肌肉和胶原骨的刚性匹配的PAAm凝胶可分别促进人间充质干细胞(hMSC)的神经源性分化、成肌分化和成骨分化[28]。同时，大量的研究显示，细胞反应对纳米拓扑结构高度敏感[34–39]。基质的纳米拓扑结构除了对细胞形态具有显著影响，还可以调节细胞增殖，并促进干细胞分化为特定的细胞谱系，如神经元[35,40,41]、肌肉[42]和骨骼[36,37]。

许多优秀的综述文章讨论了细胞对基质刚性[14,43,44]或纳米拓扑结构[45–50]的反应。然而，还未有人对基质刚性和纳米拓扑结构与细胞行为的交织影响进行充分描述[51]。本文首先综述了基质刚性和纳米拓扑结构对细胞行为的影响，然后聚焦于生物物理信号从整合素到细胞核的细胞内传递，并尝试将细胞行为的细胞外调节与基质的生物物理学特征联系在一起。最后，我们讨论了在剖析细胞行为的生物物理调节和将基质的刚性和纳米拓扑结构生物力学特性转化到组织工程和再生医学时存在的挑战。

2. 细胞表型和功能的生物物理调节

2.1. 刚性

用于细胞研究的基质材料十分广泛，这些材料刚性各有不同，包括非常硬的金属如氧化钛(TiO_2；杨氏模量$E \approx 150$ GPa [52])、硬玻璃(65 GPa [53])、热塑性聚合物如聚苯乙烯(PS；2.3 GPa [54])和聚乳酸–乙醇酸共聚物(PLGA；1.31 GPa [55])、弹性聚合物如聚二甲基硅氧烷(PDMS；3.4 MPa [56])和柔软的水凝胶(几帕到几千帕)，如图2(a)所示。在文献中，各种术语已被用于表征基质的力学性质，如弹性、刚性、硬度和剪切模量。弹性是材料的强度性质，而刚性是广延性质，其取决于材料、形状和边界条件。在本综述中，除了另有规定者，括号中的值均为基质的杨氏模量。

2.1.1. 刚性效应

随着基质刚性的增加，细胞的黏附性增强[57–60]，细胞铺展程度随肌动蛋白组织性增强而增大[60–67]，收缩力增加[60–68]，迁移速度降低[69,70]，增殖加快[57,61,67,71,72]。例如，当hMSC黏附在胶原蛋白I修饰的PAAm凝胶上时，桩蛋白标记的黏附性发生如下改变：从检测不到的软凝胶(1 kPa)上的扩散斑复合物，变为在具有中等刚性凝胶(11 kPa)上的点状黏附，直至更稳定黏附于最硬凝胶(34 kPa)上的黏着斑[28]。当藻酸盐凝胶刚性从20 kPa增加到110 kPa时，凝胶上MC3T3-E1成骨细胞中黏着斑蛋白vinculin的表达增加了1.5倍[57]。与较软(刚性较低)的凝胶相比，较硬(刚性较高)的胶原蛋白I包被的PAAm凝胶(7.69 kPa)上的NIH 3T3成纤维细胞更分散，且附着性更好；离心后，其表面的附着细胞仍剩余>80%，而更软的凝胶(2.68 kPa)上只剩下约30%的细胞[58]。

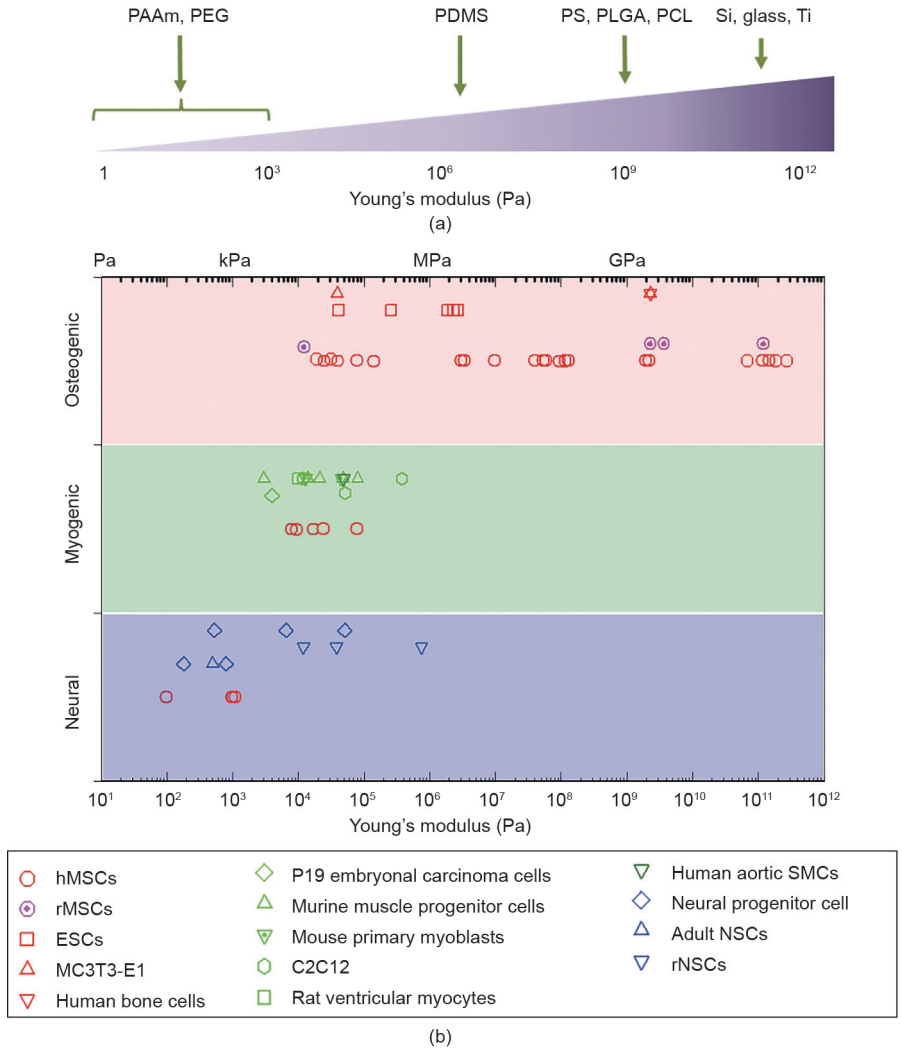

图2. 基质刚性影响细胞增殖。(a)不同刚性的细胞培养基质。(b)干细胞分化与基质刚性的关系图，图中每一种符号代表一种细胞类型。PEG：聚乙二醇；PCL：聚己内酯；rMSC：大鼠间充质干细胞；ESC：胚胎干细胞；SMC：平滑肌细胞；NSC：神经干细胞；rNSC：大鼠神经干细胞。

虽然许多研究表明，细胞行为单向依赖于基质刚性，但已有研究表明，细胞黏附[73]、迁移[59,74–76]和增殖[77–79]与基质刚性间存在双相关系。一方面，当原代成人真皮成纤维细胞在聚乙二醇(PEG)水凝胶上生长时，细胞迁移平均速度从软凝胶(95 Pa)上的0.81 μm·min^{-1}明显降低至硬凝胶(4.3 kPa)上的0.38 μm·min^{-1} [70]。此外，当PAAm凝胶的杨氏模量从4.7 kPa增加到14 kPa时，NIH 3T3成纤维细胞在24 h和48 h后细胞增殖分别达到约2倍和4倍[61]。另一方面，在胶原蛋白密度较低时，MC3T3-E1细胞在胶原蛋白I包被的PAAm凝胶上的迁移速度随刚性单调递增；而在胶原蛋白密度较高的条件下，细胞迁移速度对基质刚性的依赖呈双相性，在21.6 kPa的凝胶上达到最大值[59]。培养于中等刚性PEG凝胶基质(10 Pa~10 kPa)上的大鼠神经干细胞的增殖率达到峰值[78]。此外，藻酸盐水凝胶上鼠类干细胞的增殖对凝胶刚性无依赖性[72]。

干细胞分化也明显受基质刚性的影响。如前所述，在与脑(0.1~1 kPa)、肌肉(8~17 kPa)和胶原骨(25~40 kPa)的刚性匹配的PAAm凝胶上培养hMSC时，神经源性、肌源性和成骨生物标志物表达上调[28]。当成体神经干细胞培养于与脑组织刚性近似的基质上时，神经元生物标志物β-微管蛋白III的表达水平可达到峰值。此外，较软的PAAm凝胶(100~500 Pa)可促进神经元分化，而较硬的基质(1~10 kPa)则导致神经胶质细胞分化[78]。细胞来源、基质制备和诱导分化的实验方法的不同使不同研究得出的最佳基质刚性也有所不同。例如，一项研究显示，PAAm凝胶上成肌分化和成骨分化达到峰值时，该凝胶的刚性分别为25 kPa和80 kPa [67]，这与以往研究[28]略有不同。尽管如此，研究者已发现一般趋势——软基质适于神经分化，硬基质更利于成骨分化，而成肌分化时基质刚性的适宜值位于两者之间[图2(b)；具体数据参见补充资料]。大量涉及不同细胞

来源的研究显示出的显著一致性强调了机械感应在干/祖细胞分化中的重要作用。

已有较多研究者对刚性对细胞行为的影响进行了研究。基质刚性影响纳米粒子的细胞摄取：软的PAAm凝胶(1.61 kPa)可降低细胞膜张力，与较硬的凝胶(3.81 kPa和5.71 kPa)[80]相比，更利于牛主动脉内皮细胞摄取PS纳米颗粒。更有趣的是，最近的研究显示，细胞可以保留来自过去培养环境中的刚性信息，并且这些先前的力学信息会影响细胞未来的命运[32,81–84]。例如，骨骼肌干细胞在硬塑料培养皿上快速失去其体内再生潜能，但在生理相关刚性与体内较为接近的软水凝胶上，可维持其自我更新和再生能力[32]。进一步研究证明，长期培养于硬PS的hMSC的成骨分化能力增强，但其仍具备可塑性，可以在没有力学刺激的情况下在硬PS表面分化为成脂和成骨细胞[82]。

2.1.2. 调节刚性时面临的挑战

细胞对基质刚性的反应并不总是一致的，甚至有时是矛盾的。一个重要的原因是调节水凝胶刚性可能会影响其表面化学性质、主链柔性和凝胶黏附配体的结合特性(除体积刚性和孔隙率外)[85–87]。已有研究表明，hMSC行为随PAAm凝胶刚性的变化而变化，但不受PDMS刚性的影响；因此推测，调节细胞行为的是凝胶上黏附的胶原蛋白I锚点的改变，而不是基质刚性本身[85]。进一步研究表明，hMSC分化受纤连蛋白应变的调节，这一调节作用不受平滑PDMS刚性的影响，而受水凝胶刚性的影响[88]。相反，最近的研究显示，即使蛋白质–基质连接物密度高达50倍，hMSC分化也不会受影响；因此，有人认为，基质刚性调节干细胞分化作用不受蛋白质拘束和多孔性的影响[89]。另一个重要的问题是，当凝胶薄时，细胞可以感应到下层水凝胶，甚至支撑基质的刚性[90–92]。据估计，细胞可以约感应到5 μm深度下的“隐藏”的基质[93]，最深可达20 μm的深度[94]。总之，水凝胶横向和纵向结构的复杂性使得剖析基质刚性在细胞调节中的作用存在难度。开发一种可以独立于其他环境变量、用于刚性研究的模型系统是非常令人期待的。

2.2. 纳米拓扑结构

细胞可以感应到表面拓扑形貌上几个纳米的变化，并积极对纳米拓扑结构的变化产生反应[38]。细胞在各种纳米拓扑结构上表现出不同的行为。虽然在物理领域中纳米尺度定义为1~100 nm的长度[95]，实际上在这里讨论的纳米拓扑结构的长度尺度扩展至超过100 nm，甚至达到亚微米范围，因为细胞可以与尺度高达几微米的ECM相互作用。

2.2.1. 纳米拓扑效应

形状(如柱、凹坑和格栅)、空间形态(特征尺寸、间距和高度)和纳米级的排列都对黏附、增殖和分化等细胞行为有着显著影响，且这种影响在不同细胞间存在差异。间充质干细胞(MSC)在直径为15~100 nm的TiO_2纳米管上表现出与在平坦的TiO_2表面上不同的细胞黏附、增殖和分化[37,96]。在小TiO_2纳米管(直径约30 nm)上，hMSC的黏附力增强。与平坦的对照基质相比，在较大纳米管(直径为70~100 nm)上，细胞伸长增加约10倍，从而诱导细胞骨架应力并趋向成骨分化[37]。除了特征尺寸，纳米拓扑结构的高度可以有效调节细胞行为[97]。在通过分层产生的随机分布的纳米岛上，与平坦的对照表面相比，多种细胞类型在浅纳米岛(11~13 nm高)上表现出更明显的黏着斑和肌动蛋白应力纤维、高度铺展的形态和更大的细胞面积[98–101]。当高度增加到约90 nm时，一些细胞如人胎成骨细胞[98]、人骨髓细胞[102]和人成纤维细胞[103]的细胞铺展形态减少，伴随肌动蛋白的扩散和应力纤维的减少。相比之下，人类内皮细胞在95 nm的纳米岛上表现为更大的片状结构和更多的应力纤维[100]。在其他系统中也观察到对纳米拓扑结构产生的细胞型特异性反应[104,105]。例如，人胚胎干细胞(hESC)在平滑表面上的增殖能力增强，且能长时间维持自我更新，但在纳米孔玻璃表面上则倾向于分化，而纳米粗糙表面相较于光滑表面，在促进NIH 3T3成纤维细胞黏附方面作用更强[105]。

与各向同性纳米拓扑结构相比，各向异性纳米拓扑结构(如纳米格栅)可以导致更小的细胞尺寸和更低的增殖速率，甚至凋亡，但能促进细胞有序排列、伸长和迁移[35,101,106–111]。与平滑对照的随机分布相比，人角膜上皮细胞的黏着斑和应力纤维沿着脊宽为70~1900 nm、节距为400~4000 nm、深度为150 nm和600 nm的硅纳米格栅排列(图3)[112]。随着脊宽增加到400 nm，黏着斑尺寸随之增大，并且在脊宽大于650 nm时保持恒定。与平滑对照表面相比，所有纳米格栅上的细胞的平均细胞面积较小，但在600 nm深的所有格栅上表现为明显伸长的形态[112]。纳米格栅诱导的细胞面积缩小导致增殖速率降低。在宽度为350 nm、间距为

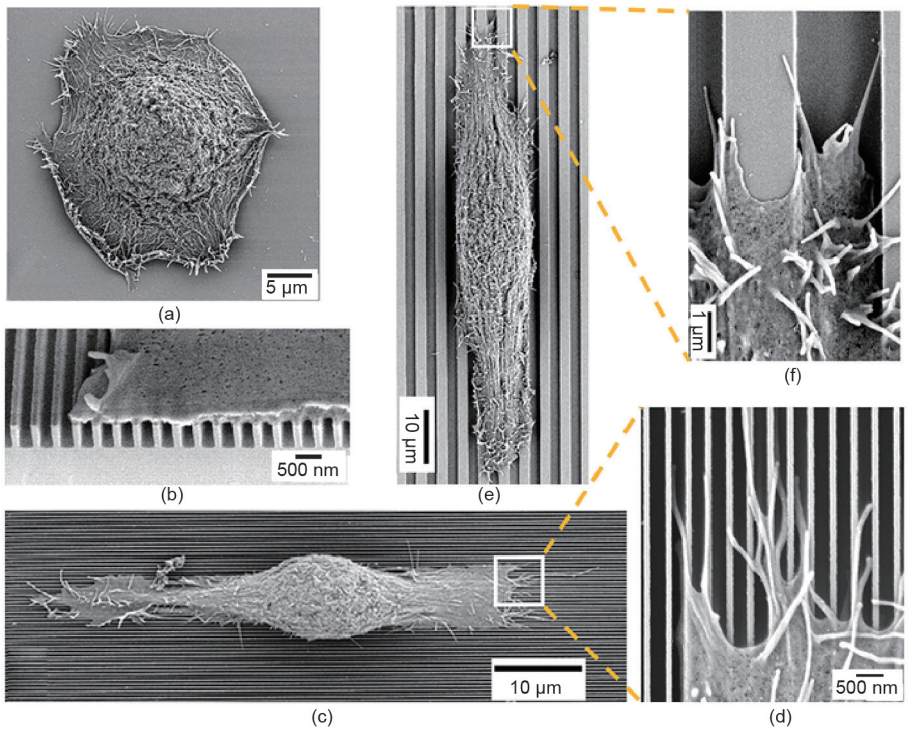

图3. 培养于(a)光滑的氧化硅基质和(b~f)纳米格栅上的人角膜上皮细胞扫描电镜图。在宽度为70 nm、间距为400 nm、深度为600 nm的纳米格栅上，细胞黏附在格栅的顶端(b)，并沿着纳米格栅结构的方向排列(c)，同时丝状伪足沿着凹槽的顶端和底端延伸(d)。相比之下，在宽度为1900 nm、间距为4000 nm、深度为600 nm的纳米格栅上，细胞伸长(e)，同时板状伪足沿着凹槽的底端延伸。图片授权改编自参考文献[112]。

700 nm、深度为350 nm的PDMS纳米格栅上，沿着纳米格栅结构的方向，hMSC的细胞骨架和细胞核明显伸长，细胞增殖率[(26.9±3.1)%]与光滑表面[(35.7±7.6)%]相比较低 [35]。除了观察到各种类型人类细胞在纳米拓扑结构上相较于光滑表面表现出更强的运动性[113–117]，在各向异性纳米拓扑结构上还可以实现定向细胞迁移，因为相较于各向同性纳米拓扑结构上的随机细胞迁移，细胞优先沿着各向异性纳米拓扑结构的长轴延伸和回缩板状伪足[118]。研究表明，定向细胞迁移可以通过微管组织中心的极化来调节[109]，且迁移速度取决于基础纳米格栅的宽度[48]和深度[119]。需要注意的是，可以通过使用纳米/微观拓扑结构梯度实现单向细胞迁移，如尺度小于单个细胞但与胶原纤维相当的锯齿几何结构[120]。

各向异性纳米拓扑结构除促进成肌分化外，对神经元生长和分化也至关重要 [42,121]。背根神经节神经元的神经突伸长，并且在定向排列的纳米纤维上没有或只有极少数分支；然而，它们在随机排列的纳米纤维上则具有更多的分支，这对神经再生是有害的。此外，这些神经突以一种与体内神经突生长方式相同的方式在与直径500 nm的纳米纤维平行的方向上形成双极延伸[122]。有趣的是，神经干细胞沿着定向排列的纳米纤维伸长和神经突的生长与纳米纤维的直径无关，但在这些纳米纤维中，直径为250 nm的纤维相较于微纤维(1.25 μm)更能促进细胞分化[123]。纳米格栅对神经元的分化有显著影响。相较于微格栅和平坦对照，在上述350 nm PDMS纳米格栅中，hMSC中神经元标志物[β-微管蛋白III和微管相关蛋白2(MAP2)]的表达显著上调。虽然纳米拓扑结构结合生物化学特性[如视黄酸(RA)]可进一步增强神经元标志物表达的上调，但是纳米格栅比单独RA处理对光滑表面的影响更大[35]。即使在未进行RA处理的情况下，生长在宽度为350 nm和高度500 nm的等间隔格栅上的hESC也能分化为神经元，而不分化为神经胶质细胞[40]。有趣的是，各向异性拓扑结构可促进神经元分化，而各向同性拓扑结构在相同条件下可促进胶质细胞分化[41]。细胞极性对细胞调节和器官发育至关重要，细胞极性的丧失与许多人类疾病有关[124,125]，各向异性纳米拓扑结构对建立和维持细胞极性而言是一种强大工具。

研究表明，纳米排列的特征对细胞表型和功能有显著影响。在正方形、六边形和接近正方形(即±50 nm无序的正方形图案)这三种不同排列的纳米凹坑阵列(直径为120 nm，中心距为300 nm，深度为100 nm)上，原代人成骨细胞在接近正方形的纳米凹坑上的原纤维黏附长

度约为11 μm，该长度明显大于在六边形和正方形纳米凹坑(约6.6 μm)和平坦对照基质(约7.2 μm)[126]上培养的细胞。此外，接近正方形的纳米凹坑能够单独刺激hMSC的成骨分化，类似于成骨诱导剂诱导分化的水平，而高度定向或完全随机定位的纳米凹坑和平坦对照基质诱导成骨分化的能力有限[36]。另一方面，高度定向的正方形纳米凹坑使hMSC的多分化潜能保留8周[39]。

作为细胞行为的有效调节剂，拓扑结构可以改变细胞–基质相互作用，从而增强或削弱细胞的黏附，最终影响细胞过程。因此，纳米拓扑结构已经应用于多个领域，从捕获循环肿瘤细胞(CTC)[127–131]、优化成纤维细胞至神经元的重编程过程[132]，直到调节成纤维细胞对纳米颗粒的纤维化反应[133]。受肿瘤细胞纳米结构表面(如微绒毛、微脊和纤毛)[134]和增强的肿瘤细胞–纳米拓扑结构相互作用的启发[135]，各种纳米拓扑结构如纳米线[127,128]、纳米管[129]和纳米级表面[130]已被用于提高CTC捕获的灵敏度和效率。与各向同性离散纳米柱相比，纳米格栅更有利于肿瘤细胞黏附和肿瘤细胞的捕获[131]。另一方面，特殊设计的纳米凹坑间距能够破坏成熟黏着斑的形成，从而有利于NIH 3T3成纤维细胞朝向更高阶区迁移[136]。由于细胞–基质相互作用减弱，纳米柱上的单层牛角膜内皮细胞的微绒毛密度比平坦对照基质的更高，且形态和功能类似于天然角膜内皮的结构[137]。

2.2.2. 细胞对纳米拓扑结构的感应

研究结果的差异混淆了我们对纳米拓扑结构调节细胞行为的理解。例如，一组研究表明，纳米格栅显著提高hMSC中成骨标志物的表达[138,139]。相反，另一组研究显示，纳米格栅对hMSC成骨表型的影响并不明显[140]。此外，一些研究者认为，相较于纳米拓扑结构，基质的生物化学性质对细胞行为的影响更为明显[107,141,142]。例如，在19~920 nm孔径梯度和正交的环状精氨酸–甘氨酸–天冬氨酸(Arg-Gly-Asp或RGD)配体梯度的硅基质上，大鼠MSC对纳米拓扑结构和生物化学性质产生反应，且这种反应在RGD密度发生变化时更为明显(相较于孔径变化时)[141]。还有研究显示，MC3T3-E1细胞主要沿着均匀包被了纤连蛋白的纳米格栅(宽度、间距和深度均为100 nm)排列。然而，当纳米格栅与10 μm厚、通过非黏性泳道分离的纤连蛋白通道正交接触印刷时，细胞沿着纤连蛋白通道而不是纳米格栅伸长[107]。目前尚不清楚上述差异是源自纳米格栅本身，还是纳米格栅改变导致的配体提呈。

通常认为纳米拓扑结构可以增加表面积，从而增强细胞黏附力。然而，细胞可以感应的表观表面大小由纳米级特征的形状和尺寸决定。细胞膜是否跨越顶部或到达纳米特征的底部取决于纳米尺度的细胞膜的刚性[143]。在等间距、高度为500 nm的纳米格栅上，新生大鼠心室肌细胞向格栅底部延伸，但达不到400 nm宽格栅的底部；这种作用伴随着有限的细胞–基质黏附力。相比之下，细胞可以完全填充800 nm宽的格栅，并且细胞–基质黏附力增强[144]。

当纳米拓扑结构减少细胞可以感应的表观表面积时，该结构限制了黏着斑的大小，从而削弱了细胞黏附，但促进了细胞迁移[102]。在直径为700 nm、柱间距离为1.2~5.6 μm的纳米柱上，hMSC被拉伸，较远的柱间距离(5.6 μm)的纳米柱有利于骨生成，较近距离(1.2 μm)的纳米柱有利于脂肪形成[145]。细胞铺展与间距之间的关系可以是双相的。例如，在直径为10~200 nm、间距为20~200 nm的纳米点阵列中，心脏成肌细胞在50 nm的纳米点阵列上的表面积和增殖能力最大[146]。另外，在直径为150 nm、400 nm和600 nm的纳米点阵列中，hMSC的成骨分化在400 nm的点阵列上达到峰值[147]。因此推测，纳米拓扑结构对细胞产生有效调节作用的决定性因素包括：纳米拓扑结构是否能增加细胞可感应的基质表面积；基质表面积增加程度是否明显。小间距可限制表观表面积，而大间距可以减少表观表面积的增加。因此，纳米拓扑结构的高度与间距的纵横比与一维参数相比可提供更全面的表征[41,50,148–151]。已有研究表明，在宽度和间距为1~10 μm，高度为0.35~10 μm的格栅上，大部分hMSC可以在纵横比为1.04的格栅上伸长，而细胞伸长现象在宽度最小或高度最大的格栅上并不明显[152]。

尽管纳米拓扑结构通过调节细胞形状可有效调节细胞生长和分化[153,154]，但其潜在机制仍不清楚。当纳米拓扑结构不影响黏附配体提呈时，纳米拓扑结构会通过接触引导影响细胞行为吗？当纳米拓扑结构影响细胞对基质表面或黏附配体的感应时，纳米拓扑结构会影响细胞行为吗？

2.3. 编织基质纳米拓扑结构和刚性

细胞不断地对ECM施加力，重塑ECM，并影响生物体的生理和病理过程[155–157]。当使用平坦、柔韧的基质时，细胞可以感知到基质刚性的差异，并对刚性

产生反应[158]。此外，当在细胞不能使之变形的刚性基质上制备拓扑结构时，细胞将仅对拓扑结构产生反应；而如果细胞可以使拓扑结构变形，则细胞将对拓扑结构和刚性均有感知和响应。需要注意的是，基质刚性感应也是细胞类型特异性的。例如，牛肺动脉平滑肌细胞在宽度、间距和深度均为350 nm的聚甲基丙烯酸甲酯(PMMA)和PDMS纳米格栅上表现相似[109]。然而，hMSC使PDMS纳米格栅变形，而不影响PS纳米格栅，PS纳米格栅(2.3 GPa)具有与PMMA纳米格栅(3.7 GPa [54])相似的刚性，如图4(a, b) 所示[159]。此外，在PS基质上，相较于平坦对照基质，当hMSC黏附到350 nm的格栅上时表现出较低的力学性能。另一方面，在PDMS基质上培养的hMSC的力学性能比PS基质更低，该现象与拓扑结构无关[160]。显然，当拓扑结构的构建材料足够柔软，使细胞能够引起基质变形时，拓扑结构和硬(刚)度交织影响着细胞表型和功能[161]。值得注意的是，通常小于100 nm长度尺度的热塑性聚合物的表面具有与本体不同的性能[162–165]。因为纳米特征构成表面区域的显著部分，因此可提供不同的力学性能，纳米拓扑结构可以为细胞提供除拓扑形貌之外的刚性。

最近开发的微尺度PDMS柱阵列提供了关于细胞对拓扑形貌和刚性反应的可靠证据[166,168–175]。柱的弹簧常量与直径的四次方成正比，与高度的立方成反比[166]。微柱阵列的设计尺寸不同，其刚性会在1 kPa~1.2 MPa范围内变化，从而影响黏着斑、细胞形态、收缩性和分化[174,176]。例如，hMSC在不同刚性的微

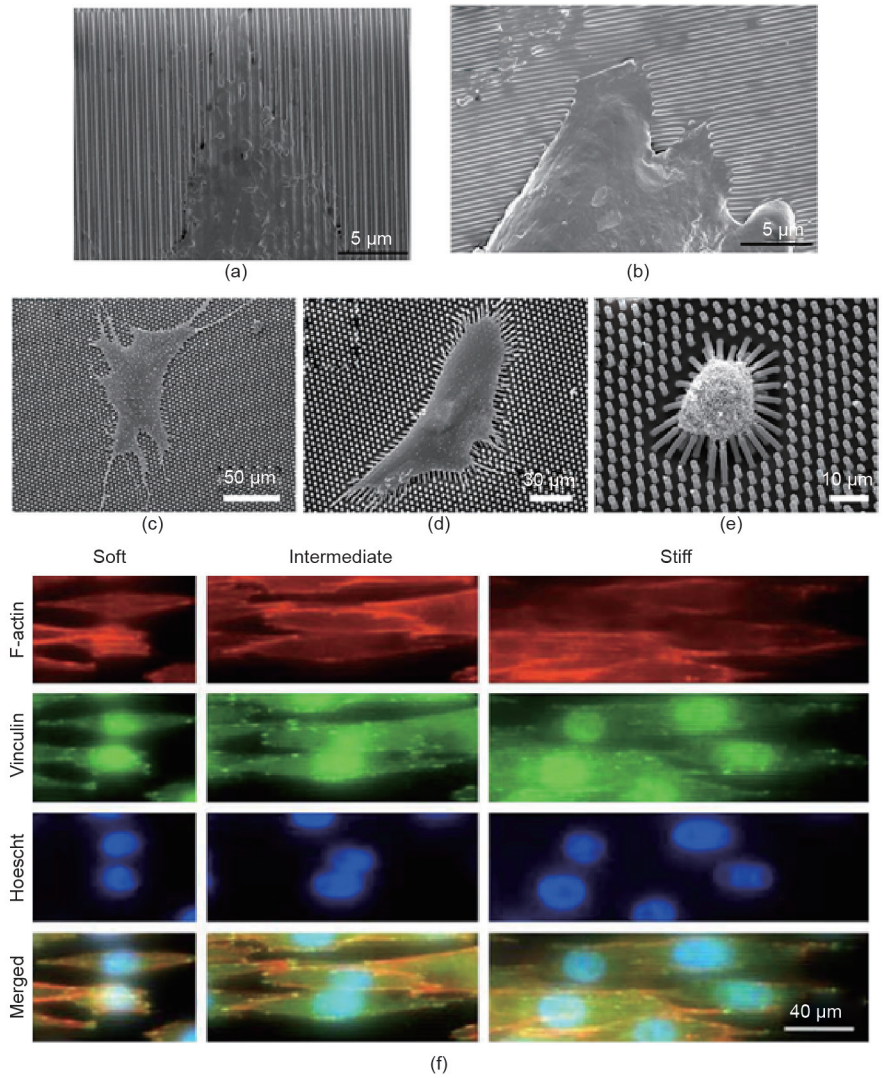

图4. 基质结构形态与刚性对细胞的交织影响。(a, b) hMSC在(a)硬质PS和(b)柔性PDMS纳米格栅上的SEM图像。(c–e) hMSC在高度分别为(c) 0.97 μm、(d) 6.1 μm 和(e) 12.9 μm的PDMS微柱阵列上的SEM图像。hMSC在图(c)所示的高度为0.97 μm的微柱阵列上铺展良好，而在图(e)所示的高度为12.9 μm的微柱阵列上呈现出带有明显明显微绒毛的圆形形态。(f)在不同刚性纳米格栅上生长的中国仓鼠卵巢(CHO)细胞的免疫荧光图像。肌动蛋白显示为红色，黏着斑蛋白显示为绿色，核物质显示为蓝色。图(a)和(b)授权改编自参考文献[159]，图(c~e)授权改编自参考文献[166]，图(f)授权改编自参考文献[167]。

柱阵列上表现出不同的细胞铺展性，如图 4(c~e)所示[166]，其对hMSC分化的影响也不同：硬(度高)的阵列有利于骨生成，而软的阵列可促进脂肪生成[166]。使用各向异性微柱阵列的细胞研究进一步强调了基质刚性的重要性。在椭圆形横截面(长轴/短轴：0.95 μm/0.55 μm，导致柱在长轴方向的刚性是短轴方向的3倍)的各向异性PDMS微阵列上，上皮细胞优先沿着长轴方向或最硬方向排列和迁移[173]。黏着斑和肌动蛋白应力纤维、细胞迁移和组织生长沿着这些基质最硬的方向优先取向，这与细胞组件边缘的更大牵引力相关[44]。相比之下，在圆柱形柱阵列上未观察到细胞排列或组装的优先取向[170]。此外，在宽度、间距和深度均为800 nm，具有1.8 MPa~1.1 GPa不同杨氏模量的聚氨酯纳米格栅上，随着基质刚性的增加，中国仓鼠卵巢(CHO)细胞铺展性和伸长性逐渐增强，细胞和核区面积逐渐增大，如图4(f)所示[167]。

基质刚性和纳米拓扑结构在细胞调节中的作用难以捉摸，交织的生物物理学特性增加了研究的复杂性。为了便于理解生物物理调节的机制，我们接下来讨论在细胞调节方面的细胞内和细胞外转导的生物物理信号的一些共同要素。

3. 生物物理信号的细胞内转导

生物物理信号可以从整合素通过黏着斑和肌动蛋白细胞骨架传递到细胞核，并调节细胞表型和功能。因此，我们关注生物物理信号如何影响黏着斑、细胞骨架和细胞核。

在讨论生物物理信号如何影响细胞之前，我们将描述细胞如何对基质产生感知和响应。细胞对基质产生反应的第一步是通过整合素结合并聚集到基质上的黏附配体形成黏着斑。如图5所示，含有一个α亚基和一个β亚基的异源二聚体整联蛋白受体与ECM蛋白的RGD肽及其细胞外结构域结合，并与细胞骨架衔接体蛋白质及其细胞质尾部连接，随后募集将整合素连接至肌动蛋白细胞骨架的支架蛋白[177]。整合素介导最早的接触形式是黏着复合物。这些小(约500 nm)但高度动态的黏着复合物位于片状伪足和膜突起的前缘[178]。当片状伪足缩回或停止突起时，黏着接触点被黏着斑替代，并且包括桩蛋白、黏着斑蛋白和踝蛋白在内的胞质锚蛋白被募集到黏附位点[179]。由肌动蛋白与肌球蛋白丝(肌动球蛋白)的交联作用驱动的细胞骨架张力能够诱导从初期的黏着复合物到稳定的条状黏着斑和纤维性粘连的成熟过程[180]。黏着斑的高度各向异性生长取向于细胞骨架施加的力的方向[181]。小GTP酶的Rho家族蛋白的下游信号随后产生[43,182]，从而调节纳米感应(Cdc42)、应力纤维形成(RhoA)和细胞铺展(Rac)[183]。然后这些进程通过蛋白质(如肌球蛋白)控制丝状肌动蛋白纤维的伸长和收缩[184]。 RhoA活性的增强可降低Cdc42和Rac的活性，驱动黏着斑和肌动蛋白应力纤维的形成[178]。基质刚性和纳米拓扑结构变化可以调节黏着斑的大小和

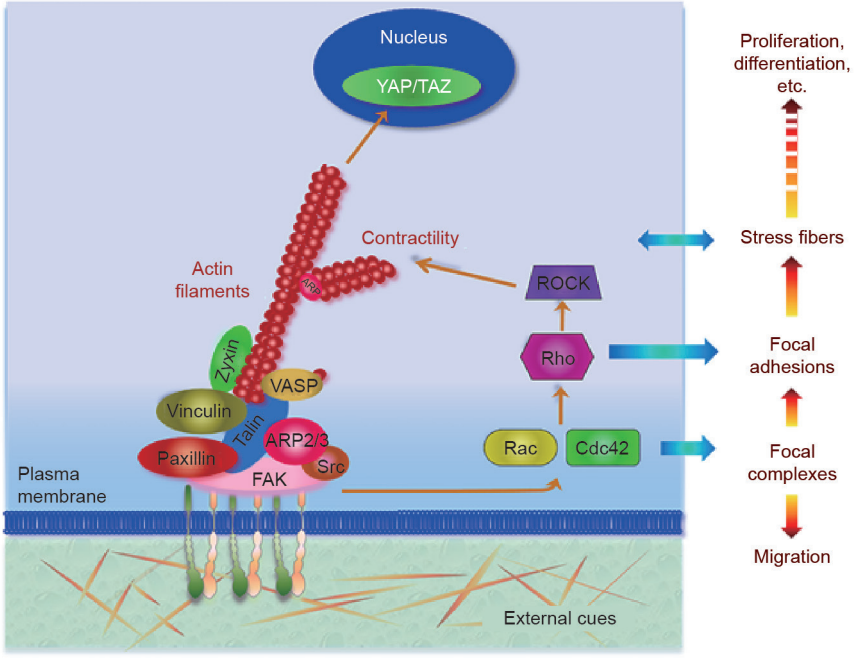

图5. 从整合素通过黏着斑和细胞骨架传递到细胞核的生物物理信号传递。ARP：肌动蛋白相关蛋白；FAK：黏着斑激酶；ROCK：Rho相关蛋白激酶；TAZ：PDZ结合模式下的转录共激活因子；VASP：血管扩张刺激磷蛋白；YAP：Yes相关蛋白。

分布，从而调节细胞骨架构成和张力，最终调节细胞形态和功能。

最近的一项研究表明，最小尺寸为0.19 μm^2 [185]的初期黏着复合物对机械感应很关键[186]。与黏着复合物一致，稳定的整合素–纤连蛋白簇在大于0.11 μm^2的面积阈值时进行组装；低于这个阈值则无法组装成稳定的整合素–纤连蛋白簇或产生明显的黏附力[187]。黏着斑的大小不能预测黏附处的局部张力。当黏着斑处施加的力持续增加时，伸长的黏附蛋白桩蛋白仍保持在细胞周边的8 μm内，尺寸没有进一步的改变[188]。作为黏着斑信号的主要调节者，黏着斑激酶(FAK)调节细胞的增殖[189]和分化[190,191]，并且其活化作用随机械应变增强[192]。通过FAK和Src介导桩蛋白磷酸化的方法，通过肌球蛋白依赖性张力将黏着斑蛋白募集至黏着斑，进一步稳定黏附[193]。事实上，FAK的酪氨酸磷酸化和脱磷酸化在细胞对基质刚性[194]和纳米拓扑结构变化的响应中起关键作用[160]。在影响ECM时，FAK信号被抑制且细胞内张力减小[195]。随着基质刚性的增加，成熟黏着斑蛋白的表达上调[56]。FAK磷酸化在宽度分别为250 nm[196]和500 nm[160]的等距纳米格栅上有所增加。磷酸化FAK(pFAK)表达的增加促进了hMSC的神经分化，这表明FAK的磷酸化可以充当整合素和细胞骨架之间的信号转导器，以便通过细胞内收缩将纳米拓扑结构刺激传递到细胞核[196]。此外，斑联蛋白的表达在350 nm的纳米格栅上下调，这与较小的[(3.2±0.26) μm^2 对(5.3±0.55) μm^2平坦对照基质]和更动态的黏着斑相关，从而表明纳米格栅上黏着斑的牵引力下降。结果hMSC以15.6 $\mu m \cdot h^{-1}$的速度沿着纳米格栅方向迁移，这明显快于其在平坦基质表面上的速度(8.3 $\mu m \cdot h^{-1}$)[197]。

黏着斑的组装取决于肌动蛋白细胞骨架的细胞内张力，并受其调节[198]，GTP酶的小Rho家族成员是肌动蛋白细胞骨架重塑的主要调节者[199]。激活Rho及其下游效应器Rho相关蛋白激酶(ROCK)，从而抑制肌球蛋白轻链磷酸酶，可促进肌动蛋白应力纤维的收缩[200]。通过ROCK依赖性收缩，肌动蛋白细胞骨架在调节细胞形状方面起主导作用，被证明能有效调节细胞生长和分化[201–203]。当微图案尺寸减小时，局限于微影图像蛋白上的细胞从生长转变为细胞凋亡[153]。铺展性良好且扁平的hMSC有利于骨生成，而未铺展且呈圆形的细胞则向成脂分化方向发展[57,59,203]。hMSC形状依赖性分化研究结果表明，在分化过程中黏着斑和肌球蛋白产生的细胞内张力在干细胞定型方面发挥关键作用[204]。铺展性好的极化形状与高RhoA/ROCK活性相关，而小且圆的细胞中RhoA/ROCK活性则较低[154]。药理学药物研究进一步证实，细胞内张力的增大能够驱动大多数hMSC向成骨细胞方向分化，尽管形状各异；相反，抑制ROCK活性则促进成脂分化[204]。此外，在成骨诱导培养基中诱导成骨分化的hMSC显示出比未分化细胞更高的细胞内张力，而在成脂诱导培养基中未分化为脂肪细胞的hMSC比在培养基中正在成脂分化的细胞收缩性更强[166]。基质刚性增加促进肌动蛋白聚合和肌动蛋白力生成，从而导致细胞内张力[205–207]和Rho活性增加，这些变化可通过降低基质刚性而减弱[21,208,209]。例如，硬的基质使RhoA和Cdc42的活化增强，从而抑制神经干细胞的神经形成，而抑制RhoA/ROCK信号传导则可适度地促进神经元分化。抑制RhoA/ROCK信号还可阻止hMSC在硬基质上的骨生成[210]。纳米拓扑结构的尺寸(特别是高度)和形状会影响细胞内张力。在多种纳米拓扑结构上检查时发现，人肺成纤维细胞在浅纳米拓扑结构(150 nm高)上显示出比在560 nm对照上更硬的细胞骨架。与具有相同尺寸和高度以及相似间距的纳米柱相比，纳米格栅还可增加细胞骨架刚性。刚性更高的细胞骨架与胶原蛋白I的合成增加有关[211]。纳米格栅还可诱导肌动球蛋白收缩性增强，这对于hESC的神经分化很关键[212]。

黏着斑、细胞骨架和细胞核之间的分子连接与细胞和核结构相关[197,213,214]，这使细胞行为的生物物理调节成为可能[215,216]。例如，鼠MSC的软骨形成需要圆形细胞，并且通过比较细胞和核形状发现，更圆的核形状与MSC中软骨形成生物标志物的最大表达相关[217]。核的可塑性与干细胞/祖细胞的定型密切相关[218]。由细胞形态调节的核变形不仅受其内容物影响，而且还受肌动蛋白细胞骨架的结构影响[219]，这种核变形可以导致染色质结构和组织中的构象适应，从而影响转录调节[220]、基因表达和蛋白质合成[216,221]，最终导致增殖、分化或细胞死亡[159,218]。将圆形细胞的铺展面积从300 μm^2增大到2500 μm^2导致G_1期细胞的核体积增加36%，细胞硬化50倍，增殖率增加10倍[222]。据推测，基质刚性和(或)纳米拓扑结构的变化可以改变黏着斑和细胞骨架的大小和分布，从而导致核变形、细胞表型和功能的变化[223]。在宽度为350 nm的等距PDMS纳米格栅上，与随机核定向和细胞伸长率为1~3的平坦对照基质相比，hMSC的细胞核优先沿着纳米格栅方向排列(62%的核)，且伸长的核也更多(伸长纵横比：1~5)。平均核面积从平坦对照基质上的(194.8±4.8) μm^2减小到纳米格栅上的(145.1±4.1) μm^2 [224]。与平坦对照基质相比，纳米格栅

还可显著下调hMSC中A型核纤层蛋白和视网膜母细胞瘤蛋白的表达，从而减少细胞增殖和改变分化潜能[213]。

核因子Yes相关蛋白(YAP)和PDZ结合模式下的转录共激活因子(TAZ)在机体发育和病理过程中发挥重要作用，并介导细胞机械感应[82,225–229]。例如，在早期小鼠胚胎中，YAP从内细胞团的多能细胞的细胞核中排除[230]。小鼠ESC中YAP的敲低导致其多能分化性丧失，而YAP的异位表达则阻止了ESC的分化[231]。此外，YAP和TAZ在纤维化肺组织中显著表达[229]。小鼠中过表达YAP和TAZ的成纤维细胞的转移导致肺中明显的ECM重塑和纤维化[229]。YAP/TAZ细胞内定位和活性主要受细胞铺展和细胞骨架张力调节[225,232]。细胞铺展时会形成厚且丰富的应力纤维，从而导致YAP/TAZ脱磷酸化和核易位，这一过程伴随着细胞增殖作用增强。相反，有限的细胞铺展(紧凑和圆形形态)产生薄和不太明显的应力纤维，导致YAP/TAZ磷酸化和细胞质易位，伴随细胞增殖的抑制[226,228,233]。抑制细胞中的肌球蛋白可减少应力纤维和核YAP的表达[234]。YAP去磷酸化可被Rho而不是Rac或Cdc42抑制剂完全阻断[233]。

YAP核质定位和活性可以被细胞间接触或细胞–基质黏附介导[226,228,233]，并且对基质刚性[82,174,225,232,235]和纳米拓扑结构[196,232,234]敏感。在微型黏附方块上，YAP核质分布随方块尺寸逐渐变化。细胞主要在小方块上表达细胞质YAP，而主要在大于30 μm×30 μm和40 μm×40 μm阈值面积的方块上表达核YAP[226]。YAP/TAZ核质定位在生理相关范围(0.5~40 kPa)内依赖于基质刚性[232]。软基质诱导细胞质中YAP的表达，抑制细胞增殖[228]，促进人类多能干细胞(hPSC)分化为运动神经元或GABA能神经元[174,235]。在刚性(硬)基质或大黏附区域中生长的hMSC中，YAP/TAZ的敲低能够促其成脂分化，这一现象通常在软基质或小黏性区域上生长的细胞中可见到；此外，YAP/TAZ的过表达导致在软基质上生长的细胞行为像在刚性(硬)基质上生长的细胞[225]。此外，YAP/TAZ作为细胞内机械力变阻器，可介导不同机械力对干细胞可塑性的影响。短时间的外力刺激引发的细胞变化导致YAP的可逆性激活；然而，超过阈值的外力刺激导致YAP的组成型激活，甚至在去除外力刺激后诱导了hMSC向成骨分化[82]。相较于基质刚性的研究，纳米拓扑结构变化对YAP细胞内定位的影响还未得到充分研究[212,232]。细胞质YAP是必需的，但不足以使人诱导的多能干细胞向神经细胞方向分化，而纳米格栅诱导的细胞极性对神经分化的诱导至关重要[234]。

4. 生物物理调节作用的比较

4.1. 基质刚性与纳米拓扑结构调制的相似性

在不同刚性和纳米拓扑结构的基质上，细胞表现出不同的表型和功能。然而，细胞对生物物理信号的反应存在明显的相似性。例如，MC3T3-E1成骨细胞在不同刚性的PAAm凝胶上表现出不同的黏着斑和细胞骨架，而在最软的凝胶(11.8 kPa)上表现出弥漫的黏着斑和组织结构差的肌动蛋白细胞骨架，但在较硬的凝胶(39 kPa)上可见明显的黏着斑和成熟的肌动蛋白应力纤维，这与玻璃表面上的细胞生长相当[59]。类似地，生长在高度有序的纳米阵列上的人成骨细胞的应力纤维发育受到扰乱，但随机排列的纳米凹坑上的细胞应力纤维铺展性良好；后者细胞的生长类似于平滑对照基质上的细胞[236]。

细胞扩散和迁移的相似性在刚性和拓扑结构逐步变化的基质上较为明显。如图6(a)所示[207]，在具有软性(14 kPa)和刚(硬)性(30 kPa)区域的PAAm基质上，单独的NIH 3T3成纤维细胞容易从软侧迁移到硬侧，同时细胞面积和牵引力增加，但是细胞迁移速度降低：在软侧为(0.44±0.23) μm·min^{-1}，而在硬侧为(0.26±0.13) μm·min^{-1}。相反，当细胞从硬侧向软侧迁移时，它们在边界处转向或收缩，如图6(b)所示[207]。即使在许多细胞间接触的情况下，相较于PAAm基质较软的区域(1.8 kPa)，NIH 3T3成纤维细胞和牛肺动脉内皮细胞优先聚集在PAAm基质较硬的区域(34 kPa)中[237]。类似地，在直径为1 μm和2 μm(相应的阵列之间的刚性比约为10)的PDMS微柱的连续阵列上，来自1 μm(软)阵列的成纤维细胞探测边界，并对阵列施加更大的力，从而诱导肌动蛋白细胞骨架的极化和促进细胞向2 μm(刚性)阵列迁移，如图6(c)所示[238]。相反，2 μm阵列上的大多数细胞不向1 μm阵列迁移，如图6(d)所示[238]。此外，当两个阵列的刚性大于50 nN·μm^{-1}时，向2 μm阵列迁移的细胞减少，如图6(e)所示，这表明基质对细胞反应的影响出现在一个较小的刚性范围内[238]。

有关刚性[239,240]和拓扑结构[118,241,242] 梯度变化的细胞研究进一步表明生物物理调制的相似性。在横跨2 mm，刚性梯度在1~240 kPa之间线性变化的PAAm基质上，NIH 3T3成纤维细胞和神经母细胞瘤细胞呈圆形形态，且在较软区域具有弥漫性黏着斑，但是在较硬的区域，随着黏着斑的出现，细胞铺展性良好，如图7(a)所示[239]。细胞还从基质较软的区域向较硬的区域

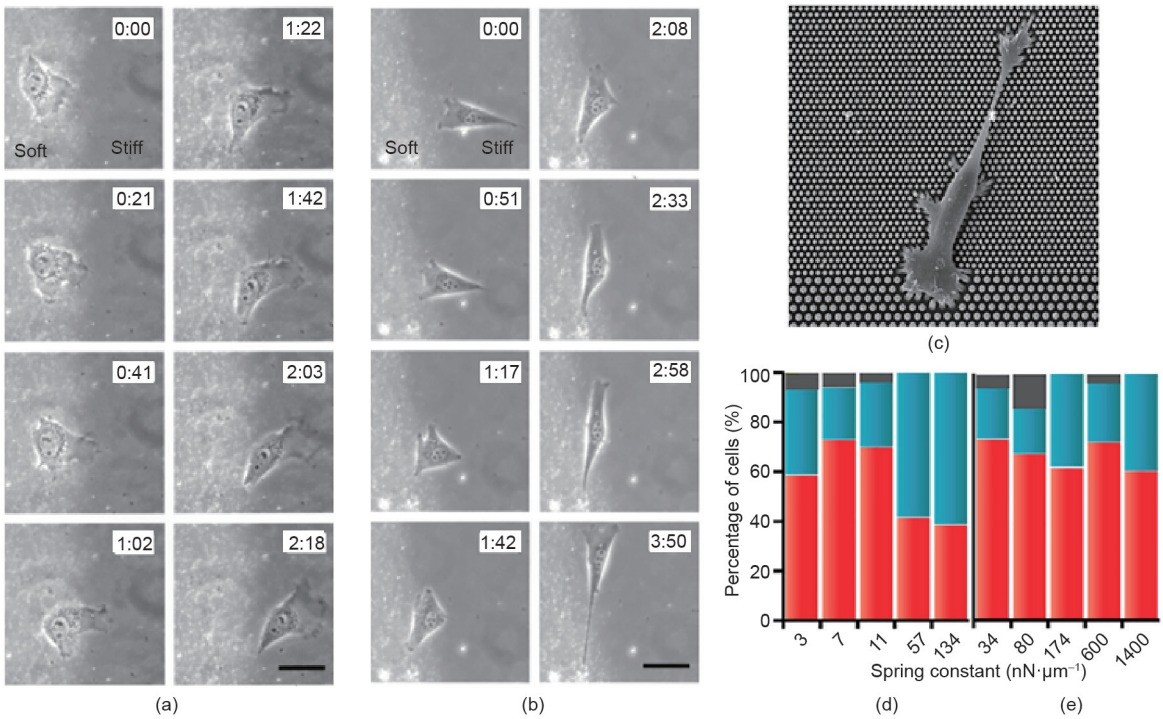

图6. 刚性和结构形态不同的基质表面细胞迁移的渐变。(a) NIH 3T3成纤维细胞从PAAm凝胶基质的软侧迁移到硬侧。(b) NIH 3T3成纤维细胞从PAAm凝胶基质的硬侧迁移到软侧。比例尺为40 μm。(c)成纤维细胞从微柱阵列直径为1 μm的区域(顶部)向直径为2 μm的区域(底部)迁移的SEM图像。微柱的密度保持不变。(d)根据直径为1 μm的微柱的弹簧常量计算细胞从1 μm阵列迁移到2 μm阵列的数量。红色柱状图：从1 μm阵列迁移到2 μm阵列的细胞占比。蓝色柱状图：未迁移的细胞占比。灰色柱状图：移动方向不明确的细胞占比。(e) 根据直径为2 μm的微柱的弹簧常量计算细胞从2 μm阵列迁移到1 μm阵列的数量。红色柱状图：2 μm阵列上迁移的细胞占比。蓝色柱状图：向1 μm阵列迁移的细胞占比。灰色柱状图：移动方向不明确的细胞占比。图(a)和(b)授权改编自参考文献[207]，图(c~e)授权改编自参考文献[238]。

迁移[240]。拓扑结构的密度也可引导细胞铺展和迁移[118,241–243]。如图7(b)所示[241]中，在*y*轴方向上具有600 nm的恒定间距，但在*x*轴方向上的间距在0.3 μm和4.2 μm之间变化的直径为600 nm的纳米柱阵列上，1205Lu黑色素瘤细胞在柱密度较稀区域上显示出长且平行的丝状伪足，而在柱密度较大区域上，则显示出短、厚且随机定向的突起。细胞迁移方向取决于柱密度和纤连蛋白密度[241]。在矩形网格阵列，NIH 3T3成纤维细胞优先迁移到网格密集区域，并远离网格稀疏的区域[242]。

最近对金纳米颗粒阵列细胞反应的研究加深了我们对基质刚性和纳米拓扑结构如何调节细胞行为的理解[244–246]。环状RGDfK肽缀合的金纳米颗粒(约8 nm)可以仅与一个约10 nm的整联蛋白分子结合[247]。使用嵌段共聚物胶束纳米光刻可控制颗粒间距，颗粒间区域通过PEG钝化消除对细胞黏附的拓扑作用[245]。各向同性配体区块间距为28~85 nm时，各种细胞类型在所有方向铺展，并当间距为58~73 nm时显示出最佳的整合素聚集、黏附、肌动蛋白应力纤维的形成和细胞铺展[245]。在具有60~110 nm的间距梯度的配体区块上，细胞清楚地感应到梯度，并向较小的间距迁移。如图7(c[i-iv])[244]所示，黏附区块间距从约50 nm增加到约80 nm，引起约Δ15 nm·mm^{-1}强度的间距梯度。细胞形态从在约50 nm间距的配体区块上的良好铺展至间距约80 nm区块上的伸长，如图7(c [v])[244]所示。另外，细胞极化并沿着间距梯度方向定向迁移[244]。不管细胞类型如何，配体间距梯度上的细胞铺展和迁移[244]与在刚性梯度[239,240]和纳米拓扑结构梯度[241,242]基质上的表现惊人的相似，从而表明基质刚性和纳米拓扑结构可能通过共同的作用途径调节细胞行为。

因此，我们假设生物物理信号调节主要通过调节基质上的黏附位点而发生。基质(通常是水凝胶)刚性水平的调节是通过改变交联密度，增加水凝胶刚性以缩小网孔尺寸来实现的。当PAAm凝胶的刚性从2 kPa增加到20 kPa时，平均孔径从15 nm减小到5.8 nm [85]。如果将黏附配体，如RGD，掺入水凝胶链中，更硬的基质可以提供更多的黏附位点，而更软的基质形成的黏附位点较少。当黏附蛋白共价接枝到水凝胶上时，网孔尺寸的增大导致锚定蛋白纤维的长度增加，从而迅速降低黏附强度和细胞对整联蛋白连接的机械反馈[85]。在纳米拓扑结构下，纳米级特征的形状、尺寸(维度)和排列决定了黏附蛋白的分布甚至构象，从而限制黏附位点进入细

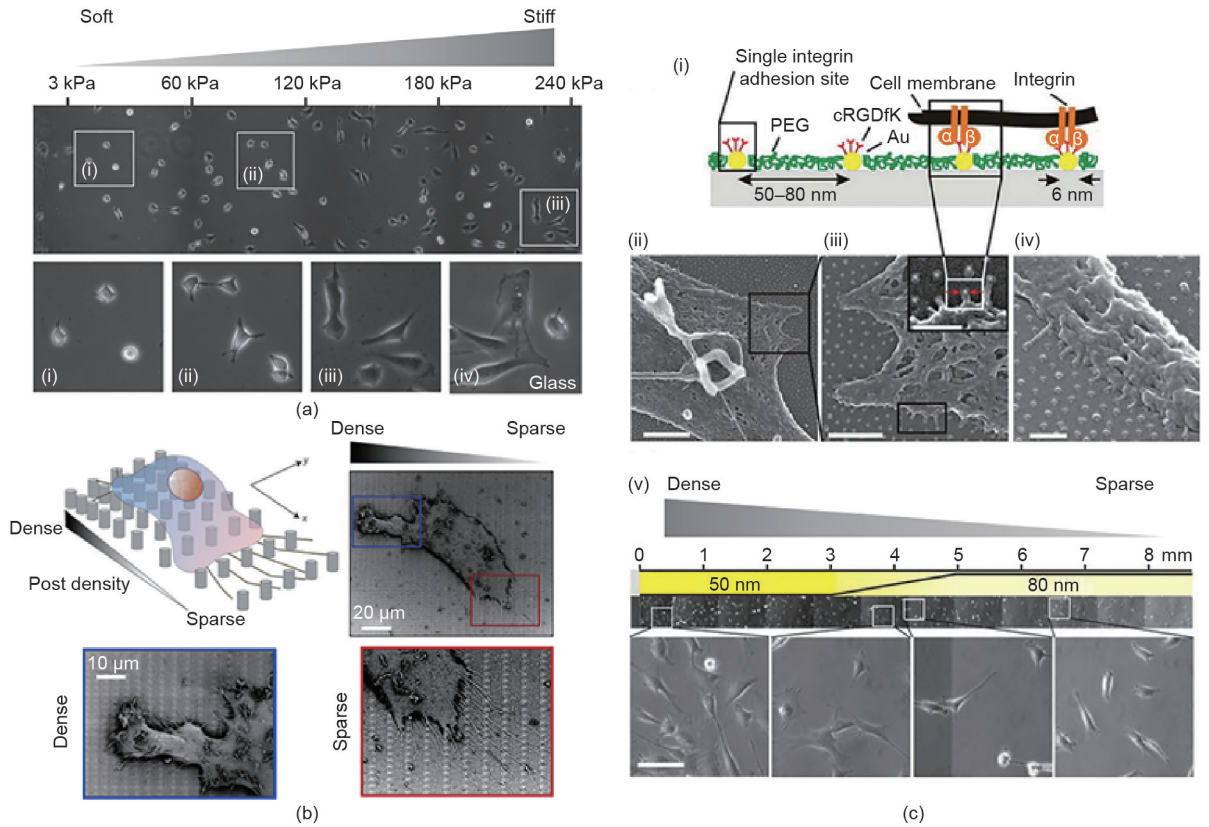

图7. 基质刚性、纳米拓扑结构、金纳米颗粒阵列梯度变化下的细胞反应。(a) NIH 3T3成纤维细胞在具有刚性梯度的水凝胶基质上的相位衬图。基质刚性在顶部给出，方框内的图像的放大图像分别为图(i~iii)。图(iv)显示了细胞在玻璃上的铺展情况。(b) 上部图片分别为1205Lu黑色素瘤细胞在具有密度梯度的纳米柱阵列上铺展的示意图和SEM图像；下部图片分别为上图中柱阵列的高密度区(蓝色方框)和低密度区(红色方框)中丝状伪足结构的放大示意图。(c) (i)金纳米颗粒阵列示意图。(ii, iii) MC3T3-E1成骨细胞在间距约为60 nm的金纳米颗粒阵列上的SEM图像。图(iii)中的嵌图展示了与金纳米颗粒选择性相互作用的细胞突起的特写。(iv) 40°倾斜视角下的与金纳米颗粒相互作用的细胞突起。(v) 生长在间距从约50 nm变化到约80 nm的金纳米颗粒阵列上的细胞。上部的相位衬图展示了细胞在阵列上的铺展情况，方框中间距分别约为50 nm、60 nm、70 nm和80 nm的放大图像在图片下部。比例尺：(ii) 500 nm，(iii) 200 nm (嵌图：100 nm)，(iv) 100 nm，(v) 100 mm。图(a)授权改编自参考文献[239]，图(b)授权改编自参考文献[241]，图(c)授权改编自参考文献[244]。

胞[101,115]。因此，通过以类似方式结合和聚集整合素的介导，基质刚性和纳米拓扑结构可用于调节黏着斑的组装和构架。对硬基质上具有ECM纳米图案的黏着斑几何结构进行调制可以模拟软基质，从而控制细胞铺展和分化[248]，这一过程也体现了黏附位点形成的关键作用。可以预见，在柔韧的纳米结构基质上，纳米拓扑结构可以物理性引导细胞行为，还可进一步通过使周围纳米结构变形的细胞上的机械反馈来调节刚性，从而调制细胞行为。

4.2. 理论建模

Bischofs等提出的模型可以用于描述细胞铺展和迁移的生物物理调控作用，该模型使用各向同性线弹性理论与基质的杨氏模量E和泊松比ν[249,250]。细胞主动牵引其周围的基质，并且假定细胞投入到基质上的功被最小化。细胞–基质接触在整个肌动蛋白细胞骨架中偶联，使得力平衡；只需要考虑成对的相对力。用于建立细胞位置各向异性力收缩偶极子P_{ij}(由张量$P_{ij}=Pn_in_j$表示，其中，P是偶极子强度，n是其取向)所需要的功ΔW与环境的应变u^e_{ij}成正比：

$$\Delta W = P_{ij}u^e_{ij}(\vec{r}_c) \quad (1)$$

最佳的细胞构成将使ΔW最小化。假设基质具有像弹簧常量为K的线性弹簧那样的功能，并且细胞通过单细胞–基质接触牵引基质。细胞–基质接触可以是单个微柱或微柱的一部分。细胞需要将能量$W=F^2/(2K)$投入到弹簧中以产生足够大的力F。通过使用弹性更好的弹簧(更大的K)，即使用较小的功(更小的W)也可有效地产生力。细胞通过在许多细胞–基质接触中的牵拉来探测基质，每个细胞具有不同的K(图8)[250]。在各向同性基质中，如图8(a)所示，所有的K是相等的，所有细胞–基质接触过程均类似；细胞不会优先定向并且采取圆形或星状形态，正如在各向同性排列的微米/纳米尺寸特征[98,166,170,251]和均质水凝胶上观察到的细胞铺展一

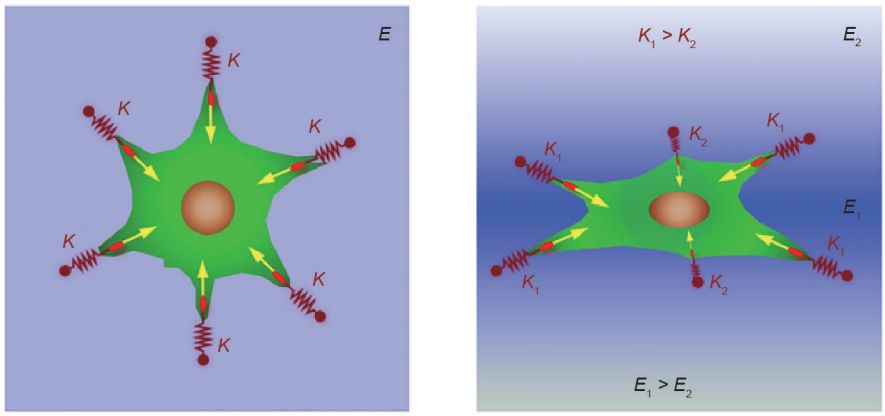

(a) (b)

图8. 机械感应影响细胞结构的机制。基质的局部弹性性质通过具有不同弹簧常量*K*的线性弹簧表示。(a)在各向同性基质中，所有的弹簧常量都相同，不同接触产生的力的大小相似，细胞不会优先定向。(b)在各向异性基质中，在弹簧常量大的接触中产生的力较大，导致细胞沿最大有效刚性的方向定向。授权改编自参考文献[250]。

样[59]。在各向异性基质中，如图8(b)所示，在一个特定方向能更有效地产生力，并且相应的接触将最终放弃其他方向。因此，基质的各向异性弹性性质可以定向那些沿着最大有效刚性的方向铺展的细胞，然后可能定向细胞运动，正如在椭圆形微柱[173]和纳米格栅[197]上，以及在具有刚性梯度的基质[240]上观察到的。值得注意的是，ΔW与基质刚性E成反比：刚性效应将仅在软性环境中发挥作用，因为刚(硬)性基质的不同接触点的ΔW差异可能变得太小，而不能诱导定向的细胞反应[250]。这解释了先前的研究结果，即一旦刚(硬)度高于某一阈值，成纤维细胞的运动对基质的渐变差异会变得不敏感[238]。

总之，实验性观察和理论分析结果提示，基质刚性和纳米拓扑结构有一些共同点；而基质刚性和纳米拓扑结构通过不同途径调节细胞行为。

5. 展望

生物物理学研究为调节细胞命运提供了机会。为了实现这种潜能，从而推进细胞工程和再生医学的发展，其关键在于剖析潜在机制，并准确地将物理刺激从二维转换到三维环境中。

5.1. 对生物物理调控机制的认识

黏附蛋白对黏附细胞感应并应答基质来说是必需的。因此，确定基质刚性和纳米拓扑结构如何影响蛋白质的吸附、构象和分布，然后确定生物物理刺激在细胞调节中的作用显得至关重要。

黏附配体和基质表面的化学活性至关重要。黏附配体对整合素黏附受体的较高亲和力有利于细胞铺展，同时增加牵引力。例如，环肽RGDfC对$\alpha_v\beta_3$整合素的亲和力比线性肽GRGDSC高约两个数量级，促进了细胞骨架收缩和hMSC的成骨分化[252]。基质表面亲水性影响蛋白质构象。胶原蛋白I折叠和聚集后，在疏水性PDMS表面上形成聚集体，从而阻碍hMSC的成骨分化；相反，这种蛋白质在亲水性PDMS表面上表现出更伸展的构象，这与$\alpha_1\beta_1$整合素的激活和成骨行为的增强相关[253]。

此外，研究表明，基质表面可以在纳米尺度有不同的表面能，从而影响黏附蛋白沉积[254–256]。纳米尺寸的金属在表面的能量比在本体中更高，这是由于在表面有更高比例的原子缺陷和离域表面电子[254,256]。聚合物表面的大分子链也显示出较高的迁移率[257,258]。表面能的变化可能导致基质蛋白质沉积的变化，并可能影响吸附的蛋白质的组成和构象，从而诱导不同的细胞反应[37,112,255,259–261]。人纤维蛋白原在直径为250 nm的PLGA柱上表现出不同于在平坦表面上的构象结构[262]。有趣的是，与最初吸附的蛋白质相比，后来出现的黏性蛋白质分子具有最高的生物活性[263]。随着基质刚性和纳米拓扑结构诱导的黏附位点的形成，区分出细胞行为的生物物理调控和生物化学调控很重要。在这方面，能够探测纳米级蛋白质的分布和构象的技术的实现令人期待[264]，例如，可达到电子显微镜的分辨率的、监测细胞对外部刺激反应的实时荧光成像系统[265]，以及可检测亚细胞区域的蛋白质活性的、具有高空间分辨率的新型生物传感器[266]。

为了确定生物物理刺激在细胞调控中的作用，建立具有单个可变基质刚性、纳米拓扑结构或生物化学特性的模型系统是必需的。目前使用的基质如水凝胶[28]和弹性体微柱阵列[166]不是理想的模型。如第2节所

述，当通过改变交联剂浓度来调节水凝胶的刚性时，体积刚性和分子尺度材料性能会发生改变[85–87]。大多数微柱阵列研究采用微尺度柱，但忽视了早期黏着复合物[186,238]。事实上，最近的研究表明，纳米柱上黏着斑的形成和黏着斑与肌动蛋白耦合的机械感应从根本上不同于微柱[171]，并且牵引力随着大于1 μm^2的黏着斑尺寸的增大而增大，而这种相关性对较小的黏着斑则不存在[169]。这些研究总体表明，纳米尺度拓扑结构可以较为真实地模拟特定刚性的连续基质。此外，弹性微柱阵列通常被氧化处理以促进蛋白质吸附，从而促进细胞黏附[166,267]。氧化过程也可能改变基质刚性[56]。肽拘束过程也可以改变基质的机械(力学)性质，使基质难以独立地调控生物物理和生物化学性质[268]。因此，含有预定的黏附配体的模型系统的建立是有好处的。小于10 nm的黏附配体应精确地定位在拓扑结构上或包埋在柔性基质中，从而使其解偶联。这需要纳米技术、材料合成和表面化学的发展。创新的纳米技术可使基质在单纳米单位内大面积图案化。嵌段共聚物胶束纳米光刻已用于控制黏附配体的位置和间距[244,245]。Dip-pen纳米光刻(DPN)已被用于直接编写整合素$\alpha_v\beta_3$纳米阵列，以研究整合素$\alpha_v\beta_3$–玻连蛋白的相互作用，从而提供了一种用于研究单一生物分子水平的细胞–基质相互作用的强力工具[269]。它也与刚性和内部配对物匹配的基质纳米级结构的制造相关[144]。此外，由于聚合物纳米结构的机械(力学)性能可能和本体显著不同，因而需要先进的测量工具横向和纵向地映射基质的纳米级性质[54,270]。

5.2. 从二维到三维的生物物理调控的转换

优化某一特定类型细胞所需基质的刚性和纳米拓扑结构的理想方法是使用高通量筛选技术。已有研究者在单一基质上制备了1~240 kPa的刚性梯度[239,240]，这涵盖了软组织的刚性(0.1~100 kPa)[11]。各种形状和尺寸(维度)的拓扑结构可以直接制造或缝合到单个平台上[41,37,271–273]，从而使在相同条件下研究拓扑构型和细胞命运决定之间的关系成为可能。

与简单的纳米拓扑结构相比，仿生基质更有吸引力，因为它可以更好地模仿天然ECM的架构，从而为细胞功能的发挥提供一个更合适的环境[274–276]。由微尺度和纳米尺度组成的分层结构也已引起研究者的兴趣[272,276–285]。微结构钛表面可促进成骨细胞的骨生成，但抑制其增殖，而微纳米复合结构则同时促进骨生成和增殖[276–278]。另一项研究表明，用250 nm格栅覆盖的微栅(宽度、高度和间距均为2 μm)利于多巴胺能神经元的产生。具有垂直排列纳米格栅的微栅能抑制星形胶质细胞的产生，但是在平行排列的纳米格栅的微栅上则观察到相反现象[272]。为了确定微拓扑结构和纳米拓扑结构所起的确切作用，研究者已经开发了诸如多纳米压印光刻(NIL)技术等新技术，以便在微图案上制造清晰的纳米拓扑结构[149,286,287]。然而，NIL需要昂贵的设备和专业知识，因此可靠但成本效益好的技术仍然是非常令人期待的，特别是那些可以生产出直接应用于临床的多层结构的技术[276]。

虽然二维体外研究有助于阐明不同基质刚性和拓扑结构下的细胞调控机制，但并不能阐释三维环境中的复杂性。因此，必须研究三维环境下的生物物理性质，以得到最有意义的结果[30,288–290]。事实上，与二维环境中的细胞相比，细胞在三维环境中显示出不同的黏附性[288]、形态[291]、增殖和分化[30,292]。例如，当在硬性凝胶顶部培养时，hMSC显示最有效的骨生成能力，而当包埋在相同的硬性凝胶中时，则主要显示为终末软骨生成能力[292]。此外，与二维条件相比，癌细胞在三维环境中显示不同的基因表达模式和对化疗药物的不同敏感性[293–296]。此外，许多生理(如形态发生和器官发生)和病理(如肿瘤发生)过程仅可在三维环境中观察到[297]。因此，已经有许多研究者努力将生物物理特性放入三维环境中进行研究。例如，研究者已经开发了共形纳米图案化技术来将黏性蛋白质图案化到形貌(拓扑结构)复杂的表面上[298]。与黏附配体共轭的金纳米颗粒在具有可调刚性的水凝胶基质上配位，包括二维凝胶[299–301]的表面和微尺寸的圆形通道的内表面[302]。基于水凝胶可以在生物条件下允许细胞被封装在内部进行加工的事实，研究者已经开发了新的策略以合成具有独立调控刚性、黏附配体和结构的水凝胶[292,303,304]。然而，保持二维基质的优点，并在生理相关刚性条件下控制所有三维环境中的拓扑和生物化学性质仍是长期存在的挑战。

人们往往忽视生物物理调控是一个动态过程的事实。细胞微环境的生物物理特性可以在发育、生理和病理过程中发生改变。ECM刚性变化的原因可能是ECM蛋白质的产生、ECM的酶降解、重塑过程的改变和矿化的程度发生变化[305]，如纤维发生期间的组织硬化[306]。最近开发的可编程材料可使细胞和生物过程对随时间而变化的刚性[307–311]、纳米拓扑结构[232,312]和基质黏附性[313]产生反应。例如，使用光诱导软化(可降解)[82]和硬化(可交联)水凝胶的研究表明，干细胞分化对动态环境敏感。

对细胞–基质相互作用(特别是在三维环境中)的全面理解不仅对阐明许多基本生物过程至关重要，而且对细胞生物处理、内源组织工程以及新一代生物材料和生物医学设备的设计十分有益。挑战越大，回报越丰厚。

致谢

作者感谢美国国家科学基金(CBET 1511759)和美国国立卫生研究院(NIH) (R15GM122953)对Yong Yang提供的资金支持，感谢NIH (HL109442, AI096305, GM110494, and UH3 TR000505)对Kam W. Leong提供的资金支持，并感谢广东省引进创新创业团队项目(2013S086)和全球实验室项目(Korean NSF GRL; 2015032163)对本研究的支持。

Compliance with ethics guidelines

Yong Yang, Kai Wang, Xiaosong Gu, and Kam W. Leong declare that they have no conflict of interest or financial conflicts to disclose.

Supplementary Information

http://engineering.org.cn/EN/10.1016/J.ENG.2017.01.014
Fig. S1
Refs. [1–35]

References

[1] Klein G. The extracellular matrix of the hematopoietic microenvironment. Experientia 1995;51(9):914–26.
[2] Shirato I, Tomino Y, Koide H, Sakai T. Fine structure of the glomerular basement membrane of the rat kidney visualized by high-resolution scanning electron microscopy. Cell Tissue Res 1991;266(1):1–10.
[3] Hironaka K, Makino H, Yamasaki Y, Ota Z. Renal basement membranes by ultrahigh resolution scanning electron microscopy. Kidney Int 1993;43(2):334–45.
[4] Abrams GA, Schaus SS, Goodman SL, Nealey PF, Murphy CJ. Nanoscale topography of the corneal epithelial basement membrane and Descemet's membrane of the human. Cornea 2000;19(1):57–64.
[5] Liliensiek SJ, Nealey P, Murphy CJ. Characterization of endothelial basement membrane nanotopography in rhesus macaque as a guide for vessel tissue engineering. Tissue Eng Part A 2009;15(9):2643–51.
[6] Kim J, Kim HN, Lim KT, Kim Y, Seonwoo H, Park SH, et al. Designing nanotopographical density of extracellular matrix for controlled morphology and function of human mesenchymal stem cells. Sci Rep 2013;3:3552.
[7] Suki B, Sato S, Parameswaran H, Szabari MV, Takahashi A, Bartolák-Suki E. Emphysema and mechanical stress-induced lung remodeling. Physiology 2013;28(6):404–13.
[8] Shvedova AA, Kisin ER, Mercer R, Murray AR, Johnson VJ, Potapovich AI, et al. Unusual inflammatory and fibrogenic pulmonary responses to single-walled carbon nanotubes in mice. Am J Physiol Lung Cell Mol Physiol 2005;289(5):L698–708.
[9] Mwenifumbo S, Stevens MM. ECM interactions with cells from the macro- to nanoscale. In: Gonsalves KE, Halberstadt CR, Laurencin CT and Nair LS, editors Biomedical nanostructures. New York: John Wiley & Sons, Inc.; 2008. p. 225–60.
[10] Silver FH, Freeman JW, Seehra GP. Collagen self-assembly and the development of tendon mechanical properties. J Biomech 2003;36(10):1529–53.
[11] Gonçalves CA, Figueiredo MH, Bairos VA. Three-dimensional organization of the elastic fibres in the rat lung. Anat Rec 1995;243(1):63–70.
[12] Ma Z, Ramakrishna S. Nanostructured extracellular matrix. Enc Nanosci Nanotechnol 2004;7:641–55.
[13] Discher DE, Mooney DJ, Zandstra PW. Growth factors, matrices, and forces combine and control stem cells. Science 2009;324(5935):1673–7.
[14] Nemir S, West JL. Synthetic materials in the study of cell response to substrate rigidity. Ann Biomed Eng 2010;38(1):2–20.
[15] Cox TR, Erler JT. Remodeling and homeostasis of the extracellular matrix: implications for fibrotic diseases and cancer. Dis Model Mech 2011;4(2):165–78.
[16] Gong H, Freddo TF, Johnson M. Age-related changes of sulfated proteoglycans in the normal human trabecular meshwork. Exp Eye Res 1992;55(5):691–709.
[17] Orr AW, Helmke BP, Blackman BR, Schwartz MA. Mechanisms of mechanotransduction. Dev Cell 2006;10(1):11–20.
[18] Wozniak MA, Chen CS. Mechanotransduction in development: a growing role for contractility. Nat Rev Mol Cell Biol 2009;10(1):34–43.
[19] Moore SW, Sheetz MP. Biophysics of substrate interaction: influence on neural motility, differentiation, and repair. Dev Neurobiol 2011;71(11):1090–101.
[20] Liu J, Tan Y, Zhang H, Zhang Y, Xu P, Chen J, et al. Soft fibrin gels promote selection and growth of tumorigenic cells. Nat Mater 2012;11(8):734–41.
[21] Paszek MJ, Zahir N, Johnson KR, Lakins JN, Rozenberg GI, Gefen A, et al. Tensional homeostasis and the malignant phenotype. Cancer Cell 2005;8(3):241–54.
[22] Parameswaran H, Majumdar A, Suki B. Linking microscopic spatial patterns of tissue destruction in emphysema to macroscopic decline in stiffness using a 3D computational model. PLOS Comput Biol 2011;7(4):e1001125.
[23] Booth AJ, Hadley R, Cornett AM, Dreffs AA, Matthes SA, Tsui JL, et al. Acellular normal and fibrotic human lung matrices as a culture system for *in vitro* investigation. Am J Resp Crit Care 2012;186(9):866–76.
[24] Liu F, Mih JD, Shea BS, Kho AT, Sharif AS, Tager AM, et al. Feedback amplification of fibrosis through matrix stiffening and COX-2 suppression. J Cell Biol 2010;190(4):693–706.
[25] Marinković A, Mih JD, Park JA, Liu F, Tschumperlin DJ. Improved throughput traction microscopy reveals pivotal role for matrix stiffness in fibroblast contractility and TGF-β responsiveness. Am J Physiol Lung Cell Mol Physiol 2012;303(3):169–80.
[26] Alenghat FJ, Ingber DE. Mechanotransduction: all signals point to cytoskeleton, matrix, and integrins. Sci STKE 2002;2002(119):pe6.
[27] Pelham RJ, Wang Y. Cell locomotion and focal adhesions are regulated by substrate flexibility. Proc Natl Acad Sci USA 1997;94(25):13661–5.
[28] Engler AJ, Sen S, Sweeney HL, Discher DE. Matrix elasticity directs stem cell lineage specification. Cell 2006;126(4):677–89.
[29] Chowdhury F, Na S, Li D, Poh Y, Tanaka T, Wang F, et al. Material properties of the cell dictate stress-induced spreading and differentiation in embryonic stem cells. Nat Mater 2010;9(1):82–8.
[30] Huebsch N, Arany PR, Mao AS, Shvartsman D, Ali OA, Bencherif SA, et al. Harnessing traction-mediated manipulation of the cell/matrix interface to control stem-cell fate. Nat Mater 2010;9(6):518–26.
[31] Holst J, Watson S, Lord MS, Eamegdool SS, Bax DV, Nivison-Smith LB, et al. Substrate elasticity provides mechanical signals for the expansion of hemopoietic stem and progenitor cells. Nat Biotechnol 2010;28(10):1123–8.
[32] Gilbert PM, Havenstrite KL, Magnusson KE, Sacco A, Leonardi NA, Kraft P, et al. Substrate elasticity regulates skeletal muscle stem cell self-renewal in culture. Science 2010;329(5995):1078–81.
[33] Engler AJ, Griffin MA, Sen S, Boennemann CG, Sweeney HL, Discher DE. Myotubes differentiate optimally on substrates with tissue-like stiffness: pathological implications for soft or stiff microenvironments. J Cell Biol 2004;166(6):877–87.
[34] Silva GA, Czeisler C, Niece KL, Beniash E, Harrington DA, Kessler JA, et al. Selective differentiation of neural progenitor cells by high-epitope density nanofibers. Science 2004;303(5662):1352–5.
[35] Yim EKF, Pang SW, Leong KW. Synthetic nanostructures inducing differentiation of human mesenchymal stem cells into neuronal lineage. Exp Cell Res 2007;313(9):1820–9.
[36] Dalby MJ, Gadegaard N, Tare R, Andar A, Riehle MO, Herzyk P, et al. The control of human mesenchymal cell differentiation using nanoscale symmetry and disorder. Nat Mater 2007;6(12):997–1003.
[37] Oh S, Brammer KS, Li YSJ, Teng D, Engler AJ, Chien S, et al. Stem cell fate dictated solely by altered nanotube dimension. Proc Natl Acad Sci USA 2009;106(7):2130–5.
[38] Brunetti V, Maiorano G, Rizzello L, Sorce B, Sabella S, Cingolani R, et al. Neurons sense nanoscale roughness with nanometer sensitivity. Proc Natl Acad Sci USA 2010;107(14):6264–9.
[39] McMurray R, Gadegaard N, Tsimbouri P, Burgess K, McNamara L, Tare R, et al. Nanoscale surfaces for the long-term maintenance of mesenchymal stem cell phenotype and multipotency. Nat Mater 2011;10(8):637–44.
[40] Lee MR, Kwon KW, Jung H, Kim HN, Suh KY, Kim K, et al. Direct differentiation of human embryonic stem cells into selective neurons on nanoscale ridge/groove pattern arrays. Biomaterials 2010;31(15):4360–6.
[41] Moe AAK, Suryana M, Marcy G, Lim SK, Ankam S, Goh JZW, et al. Microarray with micro- and nano-topographies enables identification of the optimal topography for directing the differentiation of primary murine neural progenitor cells. Small 2012;8(19):3050–61.

[42] Dang JM, Leong KW. Myogenic induction of aligned mesenchymal stem cell sheets by culture on thermally responsive electrospun nanofibers. Adv Mater 2007;19(19):2775–9.

[43] Discher DE, Janmey P, Wang Y. Tissue cells feel and respond to the stiffness of their substrate. Science 2005;310(5751):1139–43.

[44] Guilak F, Cohen DM, Estes BT, Gimble JM, Liedtke W, Chen CS. Control of stem cell fate by physical interactions with the extracellular matrix. Cell Stem Cell 2009;5(1):17–26.

[45] Flemming RG, Murphy CJ, Abrams GA, Goodman SL, Nealey PF. Effects of synthetic micro- and nano-structured surfaces on cell behavior. Biomaterials 1999;20(6):573–88.

[46] Stevens MM, George JH. Exploring and engineering the cell surface interface. Science 2005;310(5751):1135–8.

[47] Yang Y, Leong KW. Nanoscale surfacing for regenerative medicine. Wiley Interdiscip Rev Nanomed Nanobiotechnol 2010;2(5):478–95.

[48] Kim DH, Provenzano PP, Smith CL, Levchenko A. Matrix nanotopography as a regulator of cell function. J Cell Biol 2012;197(3):351–60.

[49] Dalby MJ, Gadegaard N, Oreffo RO. Harnessing nanotopography and integrin-matrix interactions to influence stem cell fate. Nat Mater 2014;13(6):558–69.

[50] Nguyen AT, Sathe SR, Yim EK. From nano to micro: topographical scale and its impact on cell adhesion, morphology and contact guidance. J Phys Condens Matter 2016;28(18):183001.

[51] Janson IA, Putnam AJ. Extracellular matrix elasticity and topography: material-based cues that affect cell function via conserved mechanisms. J Biomed Mater Res A 2015;103(3):1246–58.

[52] Elastic moduli data for polycrystalline ceramics [Internet]. Gaithersburg: National Institute of Standards and Technology. c2017 [cited 2017 Jan 8]. Available from: https://srdata.nist.gov/CeramicDataPortal/elasticity/TiO2.

[53] Halliday D, Resnick R, Walker J. Fundamentals of physics. 6th ed. New York: John Wiley & Sons, Inc.; 2000.

[54] Sahin O, Magonov S, Su C, Quate CF, Solgaard O. An atomic force microscope tip designed to measure time-varying nanomechanical forces. Nat Nanotechnol 2007;2(8):507–14..

[55] Leung L, Chan C, Baek S, Naguib H. Comparison of morphology and mechanical properties of PLGA bioscaffolds. Biomed Mater 2008;3(2):025006.

[56] Yang Y, Kulangara K, Lam RTS, Dharmawan R, Leong KW. Effects of topographical and mechanical property alterations induced by oxygen plasma modification on stem cell behavior. ACS Nano 2012;6(10):8591–8.

[57] Kong HJ, Polte TR, Alsberg E, Mooney DJ. FRET measurements of cell-traction forces and nano-scale clustering of adhesion ligands varied by substrate stiffness. Proc Natl Acad Sci USA 2005;102(12):4300–5.

[58] Guo W, Frey MT, Burnham NA, Wang Y. Substrate rigidity regulates the formation and maintenance of tissues. Biophys J 2006;90(6):2213–20.

[59] Khatiwala CB, Peyton SR, Putnam AJ. Intrinsic mechanical properties of the extracellular matrix affect the behavior of pre-osteoblastic MC3T3-E1 cells. Am J Physiol Cell Physiol 2006;290(6):C1640–50.

[60] Solon J, Levental I, Sengupta K, Georges PC, Janmey PA. Fibroblast adaptation and stiffness matching to soft elastic substrates. Biophys J 2007;93(12):4453–61.

[61] Wang H, Dembo M, Wang Y. Substrate flexibility regulates growth and apoptosis of normal but not transformed cells. Am J Physiol Cell Physiol 2000;279(5):C1345–50.

[62] Engler AJ, Richert L, Wong JY, Picart C, Discher DE. Surface probe measurements of the elasticity of sectioned tissue, thin gels and polyelectrolyte multilayer films: correlations between substrate stiffness and cell adhesion. Surf Sci 2004;570(1–2):142–54.

[63] Yeung T, Georges PC, Flanagan LA, Marg B, Ortiz M, Funaki M, et al. Effects of substrate stiffness on cell morphology, cytoskeletal structure, and adhesion. Cell Motil Cytoskeleton 2005;60(1):24–34.

[64] Brown XQ, Ookawa K, Wong JY. Evaluation of polydimethylsiloxane scaffolds with physiologically-relevant elastic moduli: interplay of substrate mechanics and surface chemistry effects on vascular smooth muscle cell response. Biomaterials 2005;26(16):3123–9.

[65] Collin O, Tracqui P, Stephanou A, Usson Y, Clément-Lacroix J, Planus E. Spatiotemporal dynamics of actin-rich adhesion microdomains: influence of substrate flexibility. J Cell Sci 2006;119(9):1914–25.

[66] Reinhart-King CA, Dembo M, Hammer DA. Cell-cell mechanical communication through compliant substrates. Biophys J 2008;95(12):6044–51.

[67] Rowlands AS, George PA, Cooper-White JJ. Directing osteogenic and myogenic differentiation of MSCs: interplay of stiffness and adhesive ligand presentation. Am J Physiol Cell Physiol 2008;295(4):C1037–44.

[68] Georges PC, Miller WJ, Meaney DF, Sawyer ES, Janmey PA. Matrices with compliance comparable to that of brain tissue select neuronal over glial growth in mixed cortical cultures. Biophys J 2006;90(8):3012–8.

[69] Wong JY, Velasco A, Rajagopalan P, Pham Q. Directed movement of vascular smooth muscle cells on gradient-compliant hydrogels. Langmuir 2003;19(5):1908–13..

[70] Ghosh K, Pan Z, Guan E, Ge S, Liu Y, Nakamura T, et al. Cell adaptation to a physiologically relevant ECM mimic with different viscoelastic properties. Biomaterials 2007;28(4):671–9.

[71] Mih JD, Marinkovic A, Liu F, Sharif AS, Tschumperlin DJ. Matrix stiffness reverses the effect of actomyosin tension on cell proliferation. J Cell Sci 2012;125(24):5974–83.

[72] Hsiong SX, Carampin P, Kong HJ, Lee KY, Mooney DJ. Differentiation stage alters matrix control of stem cells. J Biomed Mater Res A 2008;85(1):145–56.

[73] Gu Y, Ji Y, Zhao Y, Liu Y, Ding F, Gu X, et al. The influence of substrate stiffness on the behavior and functions of Schwann cells in culture. Biomaterials 2012;33(28):6672–81.

[74] DiMilla PA, Stone JA, Quinn JA, Albelda SM, Lauffenburger DA. Maximal migration of human smooth-muscle cells on fibronectin and type-IV collagen occurs at an intermediate attachment strength. J Cell Biol 1993;122(3):729–37.

[75] Peyton SR, Putnam AJ. Extracellular matrix rigidity governs smooth muscle cell motility in a biphasic fashion. J Cell Physiol 2005;204(1):198–209.

[76] Calve S, Simon HG. Biochemical and mechanical environment cooperatively regulate skeletal muscle regeneration. FASEB J 2012;26(6):2538–45.

[77] Boontheekul T, Hill EE, Kong HJ, Mooney DJ. Regulating myoblast phenotype through controlled gel stiffness and degradation. Tissue Eng 2007;13(7):1431–42.

[78] Saha K, Keung AJ, Irwin EF, Li Y, Little L, Schaffer DV, et al. Substrate modulus directs neural stem cell behavior. Biophys J 2008;95(9):4426–38.

[79] Boonen KJM, Rosaria-Chak KY, Baaijens FPT, van der Schaft DWJ, Post MJ. Essential environmental cues from the satellite cell niche: optimizing proliferation and differentiation. Am J Physiol Cell Physiol 2009;296(6):C1338–45.

[80] Huang C, Butler PJ, Tong S, Muddana HS, Bao G, Zhang S. Substrate stiffness regulates cellular uptake of nanoparticles. Nano Lett 2013;13(4):1611–5.

[81] Balestrini JL, Chaudhry S, Sarrazy V, Koehler A, Hinz B. The mechanical memory of lung myofibroblasts. Integr Biol 2012;4(4):410–21.

[82] Yang C, Tibbitt MW, Basta L, Anseth KS. Mechanical memory and dosing influence stem cell fate. Nat Mater 2014;13(6):645–52.

[83] Lee J, Abdeen AA, Kilian KA. Rewiring mesenchymal stem cell lineage specification by switching the biophysical microenvironment. Sci Rep 2014;4:5188.

[84] Li CX, Talele NP, Boo S, Koehler A, Knee-Walden E, Balestrini JL, et al. MicroRNA-21 preserves the fibrotic mechanical memory of mesenchymal stem cells. Nat Mater 2016. Epub 2016 Oct 31.

[85] Trappmann B, Gautrot JE, Connelly JT, Strange DG, Li Y, Oyen ML, et al. Extracellular-matrix tethering regulates stem-cell fate. Nat Mater 2012;11(7):642–9.

[86] Houseman BT, Mrksich M. The microenvironment of immobilized Arg-Gly-Asp peptides is an important determinant of cell adhesion. Biomaterials 2001;22(9):943–55.

[87] Keselowsky BG, Collard DM, García AJ. Integrin binding specificity regulates biomaterial surface chemistry effects on cell differentiation. Proc Natl Acad Sci USA 2005;102(17):5953–7.

[88] Li B, Moshfegh C, Lin Z, Albuschies J, Vogel V. Mesenchymal stem cells exploit extracellular matrix as mechanotransducer. Sci Rep 2013;3:2425.

[89] Wen J, Vincent LG, Fuhrmann A, Choi YS, Hribar KC, Taylor-Weiner H, et al. Interplay of matrix stiffness and protein tethering in stem cell differentiation. Nat Mater 2014;13(10):979–87.

[90] Lovett DB, Shekhar N, Nickerson JA, Roux KJ, Lele TP. Modulation of nuclear shape by substrate rigidity. Cell Mol Bioeng 2013;6(2):230–8.

[91] Maloney JM, Walton EB, Bruce CM, van Vliet KJ. Influence of finite thickness and stiffness on cellular adhesion-induced deformation of compliant substrata. Phys Rev E 2008;78(4):041923.

[92] Merkel R, Kirchgeßner N, Cesa CM, Hoffmann B. Cell force microscopy on elastic layers of finite thickness. Biophys J 2007;93(9):3314–23.

[93] Buxboim A, Rajagopal K, Brown AEX, Discher DE. How deeply cells feel: methods for thin gels. J Phys Condens Matter 2010;22(19):194116.

[94] Franck C, Maskarinec SA, Tirrell DA, Ravichandran G. Three-dimensional traction force microscopy: a new tool for quantifying cell-matrix interactions. PLoS One 2011;6(3):e17833.

[95] Roco MC. Nanotechnology: convergence with modern biology and medicine. Curr Opin Biotechnol 2003;14(3):337–46.

[96] Park J, Bauer S, Von der Mark K, Schmuki P. Nanosize and vitality: TiO_2 nanotube diameter directs cell fate. Nano Lett 2007;7(6):1686–91.

[97] Wang K, Bruce A, Mezan R, Kadiyala A, Wang L, Dawson J, et al. Nanotopographical modulation of cell function through nuclear deformation. ACS Appl Mater Interfaces 2016;8(8):5082–92.

[98] Lim JY, Hansen JC, Siedlecki CA, Runt J, Donahue HJ. Human foetal osteoblastic cell response to polymer-demixed nanotopographic interfaces. J R Soc Interface 2005;2(2):97–108.

[99] Lim JY, Hansen JC, Siedlecki CA, Hengstebeck RW, Cheng J, Winograd N, et al. Osteoblast adhesion on poly(*L*-lactic acid)/polystyrene demixed thin film blends: effect of nanotopography, surface chemistry, and wettability. Biomacromolecules 2005;6(6):3319–27.

[100] Dalby MJ, Riehle MO, Johnstone H, Affrossman S, Curtis ASG. *In vitro* reaction of endothelial cells to polymer demixed nanotopography. Biomaterials 2002;23(14):2945–54.

[101] Dalby MJ, Marshall GE, Johnstone HJH, Affrossman S, Riehle MO. Interactions of human blood and tissue cell types with 95-nm-high nanotopography. IEEE Trans Nanobioscience 2002;1(1):18–23.

[102] Frey MT, Tsai IY, Russell TP, Hanks SK, Wang YL. Cellular responses to substrate topography: role of myosin II and focal adhesion kinase. Biophys J 2006;90(10):3774–82.

[103] Dalby MJ, Yarwood SJ, Riehle MO, Johnstone HJ, Affrossman S, Curtis AS. Increasing fibroblast response to materials using nanotopography: morpho-

logical and genetic measurements of cell response to 13-nm-high polymer demixed islands. Exp Cell Res 2002;276(1):1–9.
[104] Csaderova L, Martines E, Seunarine K, Gadegaard N, Wilkinson CDW, Riehle MO. A biodegradable and biocompatible regular nanopattern for large-scale selective cell growth. Small 2010;6(23):2755–61.
[105] Chen W, Villa-Diaz LG, Sun Y, Weng S, Kim JK, Lam RHW, et al. Nanotopography influences adhesion, spreading, and self-renewal of human embryonic stem cells. ACS Nano 2012;6(5):4094–103.
[106] Thakar RG, Ho F, Huang NF, Liepmann D, Li S. Regulation of vascular smooth muscle cells by micropatterning. Biochem Biophys Res Commun 2003;307(4):883–90.
[107] Charest JL, Eliason MT, García AJ, King WP, Talin AA, Simmons BA. Polymer cell culture substrates with combined nanotopographical patterns and micropatterned chemical domains. J Vac Sci Technol B 2005;23(6):3011–4.
[108] Zhu B, Zhang Q, Lu Q, Xu Y, Yin J, Hu J, et al. Nanotopographical guidance of C6 glioma cell alignment and oriented growth. Biomaterials 2004;25(18):4215–23.
[109] Yim EKF, Reano RM, Pang SW, Yee AF, Chen CS, Leong KW. Nanopattern-induced changes in morphology and motility of smooth muscle cells. Biomaterials 2005;26(26):5405–13.
[110] Gerecht S, Bettinger CJ, Zhang Z, Borenstein JT, Vunjak-Novakovic G, Langer R. The effect of actin disrupting agents on contact guidance of human embryonic stem cells. Biomaterials 2007;28(28):4068–77.
[111] Bettinger CJ, Zhang Z, Gerecht S, Borenstein JT, Langer R. Enhancement of *in vitro* capillary tube formation by substrate nanotopography. Adv Mater 2008;20(1):99–103.
[112] Teixeira AI, Abrams GA, Bertics PJ, Murphy CJ, Nealey PF. Epithelial contact guidance on well-defined micro- and nanostructured substrates. J Cell Sci 2003;116(10):1881–92.
[113] Ranucci CS, Moghe PV. Substrate microtopography can enhance cell adhesive and migratory responsiveness to matrix ligand density. J Biomed Mater Res 2001;54(2):149–61.
[114] Prina-Mello A, Volkov Y, Kelleher D, Prendergast PJ. Comparative locomotory behavior of T lymphocytes versus T lymphoma cells on flat and grooved surfaces. Ann Biomed Eng 2003;31(9):1106–13.
[115] Brammer KS, Oh S, Gallagher JO, Jin S. Enhanced cellular mobility guided by TiO_2 nanotube surfaces. Nano Lett 2008;8(3):786–93.
[116] Liliensiek SJ, Wood JA, Yong J, Auerbach R, Nealey PF, Murphy CJ. Modulation of human vascular endothelial cell behaviors by nanotopographic cues. Biomaterials 2010;31(20):5418–26.
[117] Tan J, Saltzman WM. Topographical control of human neutrophil motility on micropatterned materials with various surface chemistry. Biomaterials 2002;23(15):3215–25.
[118] Kim DH, Han K, Gupta K, Kwon KW, Suh KY, Levchenko A. Mechanosensitivity of fibroblast cell shape and movement to anisotropic substratum topography gradients. Biomaterials 2009;30(29):5433–44.
[119] Lenhert S, Meier MB, Meyer U, Chi L, Wiesmann HP. Osteoblast alignment, elongation and migration on grooved polystyrene surfaces patterned by langmuir-blodgett lithography. Biomaterials 2005;26(5):563–70.
[120] Sun X, Driscoll MK, Guven C, Das S, Parent CA, Fourkas JT, et al. Asymmetric nanotopography biases cytoskeletal dynamics and promotes unidirectional cell guidance. Proc Natl Acad Sci USA 2015;112(41):12557–62.
[121] Wang PY, Thissen H, Tsai WB. The roles of RGD and grooved topography in the adhesion, morphology, and differentiation of C2C12 skeletal myoblasts. Biotechnol Bioeng 2012;109(8):2104–15.
[122] Patel S, Kurpinski K, Quigley R, Gao H, Hsiao BS, Poo MM, et al. Bioactive nanofibers: synergistic effects of nanotopography and chemical signaling on cell guidance. Nano Lett 2007;7(7):2122–8.
[123] Yang F, Murugan R, Wang S, Ramakrishna S. Electrospinning of nano/micro scale poly(*L*-lactic acid) aligned fibers and their potential in neural tissue engineering. Biomaterials 2005;26(15):2603–10.
[124] Bryant DM, Mostov KE. From cells to organs: building polarized tissue. Nat Rev Mol Cell Biol 2008;9(11):887–901.
[125] Petrie RJ, Doyle AD, Yamada KM. Random versus directionally persistent cell migration. Nat Rev Mol Cell Biol 2009;10(8):538–49.
[126] Biggs MJP, Richards RG, Gadegaard N, Wilkinson CDW, Dalby MJ. Regulation of implant surface cell adhesion: characterization and quantification of S-phase primary osteoblast adhesions on biomimetic nanoscale substrates. J Orthop Res 2007;25(2):273–82.
[127] Wang S, Wang H, Jiao J, Chen K, Owens GE, Kamei K, et al. Three-dimensional nanostructured substrates toward efficient capture of circulating tumor cells. Angew Chem Int Ed 2009;48(47):8970–3.
[128] Wang S, Liu K, Liu J, Yu Z, Xu X, Zhao L, et al. Highly efficient capture of circulating tumor cells by using nanostructured silicon substrates with integrated chaotic micromixers. Angew Chem Int Ed 2011;50(13):3084–8.
[129] Liu X, Chen L, Liu H, Yang G, Zhang P, Han D, et al. Bio-inspired soft polystyrene nanotube substrate for rapid and highly efficient breast cancer-cell capture. NPG Asia Mater 2013;5:e63.
[130] Chen W, Weng S, Zhang F, Allen S, Li X, Bao L, et al. Nanoroughened surfaces for efficient capture of circulating tumor cells without using capture antibodies. ACS Nano 2013;7(1):566–75.
[131] Shi L, Wang K, Yang Y. Adhesion-based tumor cell capture using nanotopography. Colloids Surf B Biointerfaces 2016;147:291–9.
[132] Kulangara K, Adler AF, Wang H, Chellappan M, Hammett E, Yasuda R, et al. The effect of substrate topography on direct reprogramming of fibroblasts to induced neurons. Biomaterials 2014;35(20):5327–36.
[133] Huang C, Ozdemir T, Xu L, Butler PJ, Siedlecki CA, Brown JL, et al. The role of substrate topography on the cellular uptake of nanoparticles. J Biomed Mater Res Part B 2016;104(3):488–95.
[134] Iyer S, Gaikwad RM, Subba-Rao V, Woodworth CD, Sokolov I. Atomic force microscopy detects differences in the surface brush of normal and cancerous cells. Nat Nanotechnol 2009;4(6):389–93.
[135] Fischer KE, Alemán BJ, Tao SL, Hugh Daniels R, Li EM, Bünger MD, et al. Biomimetic nanowire coatings for next generation adhesive drug delivery systems. Nano Lett 2009;9(2):716–20.
[136] Jeon H, Koo S, Reese WM, Loskill P, Grigoropoulos CP, Healy KE. Directing cell migration and organization via nanocrater-patterned cell-repellent interfaces. Nat Mater 2015;14(9):918–23.
[137] Teo BKK, Goh KJ, Ng ZJ, Koo S, Yim EKF. Functional reconstruction of corneal endothelium using nanotopography for tissue-engineering applications. Acta Biomater 2012;8(8):2941–52.
[138] Watari S, Hayashi K, Wood JA, Russell P, Nealey PF, Murphy CJ, et al. Modulation of osteogenic differentiation in hMSCs cells by submicron topographically-patterned ridges and grooves. Biomaterials 2012;33(1):128–36.
[139] Wood JA, Ly I, Borjesson DL, Nealey PF, Russell P, Murphy CJ. The modulation of canine mesenchymal stem cells by nano-topographic cues. Exp Cell Res 2012;318(19):2438–45.
[140] Janson IA, Kong YP, Putnam AJ. Nanotopographic substrates of poly(methyl methacrylate) do not strongly influence the osteogenic phenotype of mesenchymal stem cells *in vitro*. PLoS One 2014;9(3):e90719.
[141] Clements LR, Wang PY, Tsai WB, Thissen H, Voelcker NH. Electrochemistry-enabled fabrication of orthogonal nanotopography and surface chemistry gradients for high-throughput screening. Lab Chip 2012;12(8):1480–6.
[142] Yang J, Rose FRAJ, Gadegaard N, Alexander MR. A high-throughput assay of cell-surface interactions using topographical and chemical gradients. Adv Mater 2009;21(3):300–4.
[143] Ohara PT, Buck RC. Contact guidance *in vitro*: a light, transmission, and scanning electron microscopic study. Exp Cell Res 1979;121(2):235–49.
[144] Kim DH, Lipke EA, Kim P, Cheong R, Thompson S, Delannoy M, et al. Nanoscale cues regulate the structure and function of macroscopic cardiac tissue constructs. Proc Natl Acad Sci USA 2010;107(2):565–70.
[145] Ahn EH, Kim Y, Kshitiz, An SS, Afzal J, Lee S, et al. Spatial control of adult stem cell fate using nanotopographic cues. Biomaterials 2014;35(8):2401–10.
[146] Pan HA, Hung YC, Sui YP, Huang GS. Topographic control of the growth and function of cardiomyoblast H9c2 cells using nanodot arrays. Biomaterials 2012;33(1):20–8.
[147] You MH, Kwak MK, Kim DH, Kim K, Levchenko A, Kim DY, et al. Synergistically enhanced osteogenic differentiation of human mesenchymal stem cells by culture on nanostructured surfaces with induction media. Biomacromolecules 2010;11(7):1856–62.
[148] Crouch AS, Miller D, Luebke KJ, Hu W. Correlation of anisotropic cell behaviors with topographic aspect ratio. Biomaterials 2009;30(8):1560–7.
[149] Hu W, Yim EKF, Reano RM, Leong KW, Pang SW. Effects of nanoimprinted patterns in tissue-culture polystyrene on cell behavior. J Vac Sci Technol B 2005;23(6):2984–9.
[150] Fraser SA, Ting YH, Mallon KS, Wendt AE, Murphy CJ, Nealey PF. Sub-micron and nanoscale feature depth modulates alignment of stromal fibroblasts and corneal epithelial cells in serum-rich and serum-free media. J Biomed Mater Res A 2008;86A(3):725–35.
[151] Uttayarat P, Toworfe GK, Dietrich F, Lelkes PI, Composto RJ. Topographic guidance of endothelial cells on silicone surfaces with micro- to nanogrooves: orientation of actin filaments and focal adhesions. J Biomed Mater Res A 2005;75A(3):668–80.
[152] Wong ST, Teo SK, Park S, Chiam KH, Yim EKF. Anisotropic rigidity sensing on grating topography directs human mesenchymal stem cell elongation. Biomech Model Mechanobiol 2014;13(1):27–39.
[153] Chen CS, Mrksich M, Huang S, Whitesides GM, Ingber DE. Geometric control of cell life and death. Science 1997;276(5317):1425–8.
[154] McBeath R, Pirone DM, Nelson CM, Bhadriraju K, Chen CS. Cell shape, cytoskeletal tension, and RhoA regulate stem cell lineage commitment. Dev Cell 2004;6(4):483–95.
[155] Dembo M, Wang Y. Stresses at the cell-to-substrate interface during locomotion of fibroblasts. Biophys J 1999;76(4):2307–16.
[156] Calvo F, Ege N, Grande-Garcia A, Hooper S, Jenkins RP, Chaudhry SI, et al. Mechanotransduction and YAP-dependent matrix remodelling is required for the generation and maintenance of cancer-associated fibroblasts. Nat Cell Biol 2013;15(6):637–46.
[157] Ma X, Schickel ME, Stevenson MD, Sarang-Sieminski AL, Gooch KJ, Ghadiali SN, et al. Fibers in the extracellular matrix enable long-range stress transmission between cells. Biophys J 2013;104(7):1410–8.
[158] Harris A, Wild P, Stopak D. Silicone rubber substrata: a new wrinkle in the study of cell locomotion. Science 1980;208(4440):177–9.
[159] Chalut KJ, Kulangara K, Giacomelli MG, Wax A, Leong KW. Deformation of stem cell nuclei by nanotopographical cues. Soft Matter 2010;6(8):1675–81.
[160] Yim EKF, Darling EM, Kulangara K, Guilak F, Leong KW. Nanotopography-induced changes in focal adhesions, cytoskeletal organization, and mechanical properties of human mesenchymal stem cells. Biomaterials 2010;31(6):1299–306.
[161] Tzvetkova-Chevolleau T, Stéphanou A, Fuard D, Ohayon J, Schiavone P, Trac-

qui P. The motility of normal and cancer cells in response to the combined influence of the substrate rigidity and anisotropic microstructure. Biomaterials 2008;29(10):1541–51.
[162] Forrest JA, Dalnoki-Veress K. The glass transition in thin polymer films. Adv Colloid Interface Sci 2001;94(1–3):167–95.
[163] Van Workum K, de Pablo JJ. Computer simulation of the mechanical properties of amorphous polymer nanostructures. Nano Lett 2003;3(10):1405–10.
[164] Stafford CM, Harrison C, Beers KL, Karim A, Amis EJ, Vanlandingham MR, et al. A buckling-based metrology for measuring the elastic moduli of polymeric thin films. Nat Mater 2004;3(8):545–50.
[165] Stafford CM, Vogt BD, Harrison C, Julthongpiput D, Huang R. Elastic moduli of ultrathin amorphous polymer films. Macromolecules 2006;39(15):5095–9.
[166] Fu J, Wang YK, Yang MT, Desai RA, Yu X, Liu Z, et al. Mechanical regulation of cell function with geometrically modulated elastomeric substrates. Nat Methods 2010;7(9):733–6.
[167] Park J, Kim HN, Kim DH, Levchenko A, Suh KY. Quantitative analysis of the combined effect of substrate rigidity and topographic guidance on cell morphology. IEEE Trans Nanobioscience 2012;11(1):28–36.
[168] Balaban NQ, Schwarz US, Riveline D, Goichberg P, Tzur G, Sabanay I, et al. Force and focal adhesion assembly: a close relationship studied using elastic micropatterned substrates. Nat Cell Biol 2001;3(5):466–72.
[169] Tan JL, Tien J, Pirone DM, Gray DS, Bhadriraju K, Chen CS. Cells lying on a bed of microneedles: an approach to isolate mechanical force. Proc Natl Acad Sci USA 2003;100(4):1484–9.
[170] du Roure O, Saez A, Buguin A, Austin RH, Chavrier P, Siberzan P, et al. Force mapping in epithelial cell migration. Proc Natl Acad Sci USA 2005;102(7):2390–5.
[171] Ghassemi S, Meacci G, Liu S, Gondarenko AA, Mathur A, Roca-Cusachs P, et al. Cells test substrate rigidity by local contractions on submicrometer pillars. Proc Natl Acad Sci USA 2012;109(14):5328–33.
[172] Yang M, Sniadecki NJ, Chen C. Geometric considerations of micro- to nanoscale elastomeric post arrays to study cellular traction forces. Adv Mater 2007;19(20):3119–23.
[173] Saez A, Ghibaudo M, Buguin A, Silberzan P, Ladoux B. Rigidity-driven growth and migration of epithelial cells on microstructured anisotropic substrates. Proc Natl Acad Sci USA 2007;104(20):8281–6.
[174] Sun Y, Yong KM, Villa-Diaz LG, Zhang X, Chen W, Philson R, et al. Hippo/YAP-mediated rigidity-dependent motor neuron differentiation of human pluripotent stem cells. Nat Mater 2014;13(6):599–604.
[175] Han SJ, Bielawski KS, Ting LH, Rodriguez ML, Sniadecki NJ. Decoupling substrate stiffness, spread area, and micropost density: a close spatial relationship between traction forces and focal adhesions. Biophys J 2012;103(4):640–8.
[176] Saez A, Buguin A, Silberzan P, Ladoux B. Is the mechanical activity of epithelial cells controlled by deformations or forces? Biophys J 2005;89(6):L52–4.
[177] Hynes RO. Integrins: bidirectional, allosteric signaling machines. Cell 2002;110(6):673–87.
[178] Ridley AJ, Schwartz MA, Burridge K, Firtel RA, Ginsberg MH, Borisy G, et al. Cell migration: integrating signals from front to back. Science 2003;302(5651):1704–9.
[179] Zaidel-Bar R, Cohen M, Addadi L, Geiger B. Hierarchical assembly of cell-matrix adhesion complexes. Biochem Soc Trans 2004;32(3):416–20.
[180] Galbraith CG, Yamada KM, Sheetz MP. The relationship between force and focal complex development. J Cell Biol 2002;159(4):695–705.
[181] Besser A, Safran SA. Force-induced adsorption and anisotropic growth of focal adhesions. Biophys J 2006;90(10):3469–84.
[182] Riveline D, Zamir E, Balaban NQ, Schwarz US, Ishizaki T, Narumiya S, et al. Focal contacts as mechanosensors. J Cell Biol 2001;153(6):1175–86.
[183] Nobes CD, Hall A. Rho, Rac, and Cdc42 GTPases regulate the assembly of multimolecular focal complexes associated with actin stress fibers, lamellipodia, and filopodia. Cell 1995;81(1):53–62.
[184] DeMali KA, Burridge K. Coupling membrane protrusion and cell adhesion. J Cell Sci 2003;116(12):2389–97.
[185] Choi CK, Vicente-Manzanares M, Zareno J, Whitmore LA, Mogilner A, Horwitz AR. Actin and α-actinin orchestrate the assembly and maturation of nascent adhesions in a myosin II motor-independent manner. Nat Cell Biol 2008;10(9):1039–50.
[186] Plotnikov SV, Pasapera AM, Sabass B, Waterman CM. Force fluctuations within focal adhesions mediate ECM-rigidity sensing to guide directed cell migration. Cell 2012;151(7):1513–27.
[187] Coyer SR, Singh A, Dumbauld DW, Calderwood DA, Craig SW, Delamarche E, et al. Nanopatterning reveals an ECM area threshold for focal adhesion assembly and force transmission that is regulated by integrin activation and cytoskeleton tension. J Cell Sci 2012;125(21):5110–23.
[188] Stricker J, Aratyn-Schaus Y, Oakes PW, Gardel ML. Spatiotemporal constraints on the force-dependent growth of focal adhesions. Biophys J 2011;100(12):2883–93.
[189] Cary LA, Chang J, Guan J. Stimulation of cell migration by overexpression of focal adhesion kinase and its association with Src and Fyn. J Cell Sci 1996;109(Pt 7):1787–94.
[190] Xu B, Song G, Ju Y, Li X, Song Y, Watanabe S. RhoA/ROCK, cytoskeletal dynamics, and focal adhesion kinase are required for mechanical stretch-induced tenogenic differentiation of human mesenchymal stem cells. J Cell Physiol 2012;227(6):2722–9.
[191] Salasznyk RM, Klees RF, Williams WA, Boskey A, Plopper GE. Focal adhesion kinase signaling pathways regulate the osteogenic differentiation of human mesenchymal stem cells. Exp Cell Res 2007;313(1):22–37.
[192] Wang H, Dembo M, Hanks SK, Wang Y. Focal adhesion kinase is involved in mechanosensing during fibroblast migration. Proc Natl Acad Sci USA 2001;98(20):11295–300.
[193] Pasapera AM, Schneider IC, Rericha E, Schlaepfer DD, Waterman CM. Myosin II activity regulates vinculin recruitment to focal adhesions through FAK-mediated paxillin phosphorylation. J Cell Biol 2010;188(6):877–90.
[194] Provenzano PP, Inman DR, Eliceiri KW, Keely PJ. Matrix density-induced mechanoregulation of breast cell phenotype, signaling and gene expression through a FAK-ERK linkage. Oncogene 2009;28(49):4326–43.
[195] Humphrey JD, Dufresne ER, Schwartz MA. Mechanotransduction and extracellular matrix homeostasis. Nat Rev Mol Cell Biol 2014;15(12):802–12.
[196] Teo BK, Wong ST, Lim CK, Kung TY, Yap CH, Ramagopal Y, et al. Nanotopography modulates mechanotransduction of stem cells and induces differentiation through focal adhesion kinase. ACS Nano 2013;7(6):4785–98.
[197] Kulangara K, Yang Y, Yang J, Leong KW. Nanotopography as modulator of human mesenchymal stem cell function. Biomaterials 2012;33(20):4998–5003.
[198] Geiger B, Spatz JP, Bershadsky AD. Environmental sensing through focal adhesions. Nat Rev Mol Cell Biol 2009;10(1):21–33.
[199] Burridge K, Wennerberg K. Rho and Rac take center stage. Cell 2004;116(2):167–79.
[200] Tomasek JJ, Gabbiani G, Hinz B, Chaponnier C, Brown RA. Myofibroblasts and mechano-regulation of connective tissue remodelling. Nat Rev Mol Cell Biol 2002;3(5):349–63.
[201] Treiser MD, Yang EH, Gordonov S, Cohen DM, Androulakis IP, Kohn J, et al. Cytoskeleton-based forecasting of stem cell lineage fates. Proc Natl Acad Sci USA 2010;107(2):610–5.
[202] Murphy WL, McDevitt TC, Engler AJ. Materials as stem cell regulators. Nat Mater 2014;13(6):547–57. Erratum in: Nat Mater 2014;13(7):756.
[203] Wang N, Tolić-Nørrelykke IM, Chen J, Mijailovich SM, Butler JP, Fredberg JJ, et al. Cell prestress. I. Stiffness and prestress are closely associated in adherent contractile cells. Am J Physiol 2002;282(3):C606–16.
[204] Kilian KA, Bugarija B, Lahn BT, Mrksich M. Geometric cues for directing the differentiation of mesenchymal stem cells. Proc Natl Acad Sci USA 2010;107(11):4872–7.
[205] Wang JH, Lin JS. Cell traction force and measurement methods. Biomech Model Mechanobiol 2007;6(6):361–71.
[206] Ghibaudo M, Saez A, Trichet L, Xayaphoummine A, Browaeys J, Silberzan P, et al. Traction forces and rigidity sensing regulate cell functions. Soft Matter 2008;4(9):1836–43.
[207] Lo C, Wang H, Dembo M, Wang Y. Cell movement is guided by the rigidity of the substrate. Biophys J 2000;79(1):144–52.
[208] Klein EA, Yin L, Kothapalli D, Castagnino P, Byfield FJ, Xu T, et al. Cell-cycle control by physiological matrix elasticity and *in vivo* tissue stiffening. Curr Biol 2009;19(18):1511–8.
[209] Jay PY, Pham PA, Wong SA, Elson EL. A mechanical function of myosin II in cell motility. J Cell Sci 1995;108(Pt 1):387–93.
[210] Keung AJ, de Juan-Pardo EM, Schaffer DV, Kumar S. Rho GTPases mediate the mechanosensitive lineage commitment of neural stem cells. Stem Cells 2011;29(11):1886–97.
[211] Wang K, He X, Linthicum W, Mezan R, Wang L, Rojanasakul Y, et al. Carbon nanotubes induced fibrogenesis on nanostructured substrates. Environ Sci Nano 2017.
[212] Ankam S, Lim CK, Yim EK. Actomyosin contractility plays a role in MAP2 expression during nanotopography-directed neuronal differentiation of human embryonic stem cells. Biomaterials 2015;47:20–8.
[213] Kulangara K, Yang J, Chellappan M, Yang Y, Leong KW. Nanotopography alters nuclear protein expression, proliferation and differentiation of human mesenchymal stem/stromal cells. PLoS One 2014;9(12):e114698.
[214] Maniotis AJ, Chen CS, Ingber DE. Demonstration of mechanical connections between integrins, cytoskeletal filaments, and nucleoplasm that stabilize nuclear structure. Proc Natl Acad Sci USA 1997;94(3):849–54.
[215] Wormer DB, Davis KA, Henderson JH, Turner CE. The focal adhesion-localized CdGAP regulates matrix rigidity sensing and durotaxis. PLoS One 2014;9(3):e91815.
[216] Thomas CH, Collier JH, Sfeir CS, Healy KE. Engineering gene expression and protein synthesis by modulation of nuclear shape. Proc Natl Acad Sci USA 2002;99(4):1972–7.
[217] McBride SH, Knothe Tate ML. Modulation of stem cell shape and fate A: the role of density and seeding protocol on nucleus shape and gene expression. Tissue Eng Part A 2008;14(9):1561–72.
[218] Pajerowski JD, Dahl KN, Zhong FL, Sammak PJ, Discher DE. Physical plasticity of the nucleus in stem cell differentiation. Proc Natl Acad Sci USA 2007;104(40):15619–24.
[219] Sims JR, Karp S, Ingber DE. Altering the cellular mechanical force balance results in integrated changes in cell, cytoskeletal and nuclear shape. J Cell Sci 1992;103(Pt 4):1215–22.
[220] Dahl KN, Ribeiro AJ, Lammerding J. Nuclear shape, mechanics, and mechanotransduction. Circ Res 2008;102(11):1307–18.
[221] Dalby MJ, Riehle MO, Yarwood SJ, Wilkinson CDW, Curtis ASG. Nucleus alignment and cell signaling in fibroblasts: response to a micro-grooved topography. Exp Cell Res 2003;284(2):274–80.
[222] Roca-Cusachs P, Alcaraz J, Sunyer R, Samitier J, Farré R, Navajas D. Micropat-

terning of single endothelial cell shape reveals a tight coupling between nuclear volume in G1 and proliferation. Biophys J 2008;94(12):4984–95.
[223] Vogel V, Sheetz M. Local force and geometry sensing regulate cell functions. Nat Rev Mol Cell Biol 2006;7(4):265–75.
[224] Yang Y, Kulangara K, Sia J, Wang L, Leong KW. Engineering of a microfluidic cell culture platform embedded with nanoscale features. Lab Chip 2011;11(9):1638–46.
[225] Dupont S, Morsut L, Aragona M, Enzo E, Giulitti S, Cordenonsi M, et al. Role of YAP/TAZ in mechanotransduction. Nature 2011;474(7350):179–83.
[226] Wada K, Itoga K, Okano T, Yonemura S, Sasaki H. Hippo pathway regulation by cell morphology and stress fibers. Development 2011;138(18):3907–14.
[227] Zhao B, Tumaneng K, Guan KL. The Hippo pathway in organ size control, tissue regeneration and stem cell self-renewal. Nat Cell Biol 2011;13(8):877–83.
[228] Aragona M, Panciera T, Manfrin A, Giulitti S, Michielin F, Elvassore N, et al. A mechanical checkpoint controls multicellular growth through YAP/TAZ regulation by actin-processing factors. Cell 2013;154(5):1047–59.
[229] Liu F, Lagares D, Choi KM, Stopfer L, Marinkovic A, Vrbanac V, et al. Mechanosignaling through YAP and TAZ drives fibroblast activation and fibrosis. Am J Physiol Lung C 2015;308(4):L344–57.
[230] Tremblay AM, Camargo FD. Hippo signaling in mammalian stem cells. Semin Cell Dev Biol 2012;23(7):818–26.
[231] Lian I, Kim J, Okazawa H, Zhao J, Zhao B, Yu J, et al. The role of YAP transcription coactivator in regulating stem cell self-renewal and differentiation. Genes Dev 2010;24(11):1106–18.
[232] Mosqueira D, Pagliari S, Uto K, Ebara M, Romanazzo S, Escobedo-Lucea C, et al. Hippo pathway effectors control cardiac progenitor cell fate by acting as dynamic sensors of substrate mechanics and nanostructure. ACS Nano 2014;8(3):2033–47.
[233] Zhao B, Li L, Wang L, Wang C, Yu J, Guan K. Cell detachment activates the Hippo pathway via cytoskeleton reorganization to induce anoikis. Genes Dev 2012;26(1):54–68.
[234] Song L, Wang K, Li Y, Yang Y. Nanotopography promoted neuronal differentiation of human induced pluripotent stem cells. Colloids Surf B 2016;148:49–58.
[235] Musah S, Wrighton PJ, Zaltsman Y, Zhong X, Zorn S, Parlato MB, et al. Substratum-induced differentiation of human pluripotent stem cells reveals the coactivator YAP is a potent regulator of neuronal specification. Proc Natl Acad Sci USA 2014;111(38):13805–10.
[236] Biggs MJP, Richards RG, Gadegaard N, Wilkinson CDW, Dalby MJ. The effects of nanoscale pits on primary human osteoblast adhesion formation and cellular spreading. J Mater Sci–Mater Med 2007;18(2):399–404.
[237] Gray DS, Tien J, Chen CS. Repositioning of cells by mechanotaxis on surfaces with micropatterned Young's modulus. J Biomed Mater Res A 2003;66A(3):605–14.
[238] Trichet L, Le Digabel J, Hawkins RJ, Vedula SR, Gupta M, Ribrault C, et al. Evidence of a large-scale mechanosensing mechanism for cellular adaptation to substrate stiffness. Proc Natl Acad Sci USA 2012;109(18):6933–8.
[239] Sunyer R, Jin AJ, Nossal R, Sackett DL. Fabrication of hydrogels with steep stiffness gradients for studying cell mechanical response. PLoS One 2012;7(10):e46107.
[240] Zaari N, Rajagopalan P, Kim SK, Engler AJ, Wong JY. Photopolymerization in microfluidic gradient generators: microscale control of substrate compliance to manipulate cell response. Adv Mater 2004;16(23–24):2133–7.
[241] Park J, Kim DH, Kim HN, Wang CJ, Kwak MK, Hur E, et al. Directed migration of cancer cells guided by the graded texture of the underlying matrix. Nat Mater 2016;15(7):792–801.
[242] Kim DH, Seo CH, Han K, Kwon KW, Levchenko A, Suh KY. Guided cell migration on microtextured substrates with variable local density and anisotropy. Adv Funct Mater 2009;19(10):1579–86.
[243] Khung YL, Barritt G, Voelcker NH. Using continuous porous silicon gradients to study the influence of surface topography on the behaviour of neuroblastoma cells. Exp Cell Res 2008;314(4):789–800.
[244] Arnold M, Hirschfeld-Warneken VC, Lohmüeller T, Heil P, Blüemmel J, Cavalcanti-Adam EA, et al. Induction of cell polarization and migration by a gradient of nanoscale variations in adhesive ligand spacing. Nano Lett 2008;8(7):2063–9.
[245] Arnold M, Cavalcanti-Adam EA, Glass R, Blüemmel J, Eck W, Kantlehner M, et al. Activation of integrin function by nanopatterned adhesive interfaces. Chemphyschem 2004;5(3):383–8.
[246] Arnold M, Schwieder M, Blüemmel J, Cavalcanti-Adam EA, López-Garcia M, Kessler H, et al. Cell interactions with hierarchically structured nanopatterned adhesive surfaces. Soft Matter 2009;5(1):72–7.
[247] Xiong J, Stehle T, Diefenbach B, Zhang R, Dunker R, Scott DL, et al. Crystal structure of the extracellular segment of integrin αVβ3. Science 2001;294(5541):339–45.
[248] Gautrot JE, Malmström J, Sundh M, Margadant C, Sonnenberg A, Sutherland DS. The nanoscale geometrical maturation of focal adhesions controls stem cell differentiation and mechanotransduction. Nano Lett 2014;14(7):3945–52.
[249] Bischofs IB, Safran SA, Schwarz US. Elastic interactions of active cells with soft materials. Phys Rev E 2004;69(2):021911.
[250] Bischofs IB, Schwarz US. Cell organization in soft media due to active mechanosensing. Proc Natl Acad Sci USA 2003;100(16):9274–9.
[251] Dalby MJ, Biggs MJ, Gadegaard N, Kalna G, Wilkinson CD, Curtis AS. Nanotopographical stimulation of mechanotransduction and changes in interphase centromere positioning. J Cell Biochem 2007;100(2):326–38.
[252] Kilian KA, Mrksich M. Directing stem cell fate by controlling the affinity and density of ligand–receptor interactions at the biomaterials interface. Angew Chem Int Ed 2012;51(20):4891–5.
[253] Razafiarison T, Silván U, Meier D, Snedeker JG. Surface-driven collagen self-assembly affects early osteogenic stem cell signaling. Adv Healthc Mater 2016;5(12):1481–92.
[254] Siegel RW. Creating nanophase materials. Sci Am 1996;275(6):74–9.
[255] Webster TJ, Schadler LS, Siegel RW, Bizios R. Mechanisms of enhanced osteoblast adhesion on nanophase alumina involve vitronectin. Tissue Eng 2004;7(3):291–301.
[256] Puckett SD, Lee PP, Ciombor DM, Aaron RK, Webster TJ. Nanotextured titanium surfaces for enhancing skin growth on transcutaneous osseointegrated devices. Acta Biomater 2010;6(6):2352–62.
[257] Yang Y, Liu D, Xie Y, Lee LJ, Tomasko DL. Low-temperature fusion of polymeric nanostructures using carbon dioxide. Adv Mater 2007;19(2):251–4.
[258] Yang Y, Cheng MMC, Hu X, Liu D, Goyette RJ, Lee LJ, et al. Low-pressure carbon dioxide enhanced polymer chain mobility below the bulk glass transition temperature. Macromolecules 2007;40(4):1108–11.
[259] den Braber ET, de Ruijter JE, Ginsel LA, von Recum AF, Jansen JA. Orientation of ECM protein deposition, fibroblast cytoskeleton, and attachment complex components on silicone microgrooved surfaces. J Biomed Mater Res 1998;40(2):291–300.
[260] Andersson AS, Brink J, Lidberg U, Sutherland DS. Influence of systematically varied nanoscale topography on the morphology of epithelial cells. IEEE Trans Nanobioscience 2003;2(2):49–57.
[261] Choudhary S, Haberstroh KM, Webster TJ. Enhanced functions of vascular cells on nanostructured Ti for improved stent applications. Tissue Eng 2007;13(7):1421–30.
[262] Koh LB, Rodriguez I, Venkatraman SS. Conformational behavior of fibrinogen on topographically modified polymer surfaces. Phys Chem Chem Phys 2010;12(35):10301–8.
[263] Norde W, Horbett TA, Brash JL. Proteins at interfaces III: introductory overview. In: Horbett T, Brash JL, Norde W, editors Proteins at interfaces III state of the art. Washington, DC: American Chemical Society; 2012. p. 1–34.
[264] Chirasatitsin S, Engler AJ. Detecting cell-adhesive sites in extracellular matrix using force spectroscopy mapping. J Phys Condens Matter 2010;22(19):194102.
[265] Berning S, Willig KI, Steffens H, Dibaj P, Hell SW. Nanoscopy in a living mouse brain. Science 2012;335(6068):551.
[266] Grashoff C, Hoffman BD, Brenner MD, Zhou R, Parsons M, Yang M, et al. Measuring mechanical tension across vinculin reveals regulation of focal adhesion dynamics. Nature 2010;466(7303):263–6.
[267] Heil P, Spatz JP. Lateral shear forces applied to cells with single elastic micropillars to influence focal adhesion dynamics. J Phys Condens Matter 2010;22(19):194108.
[268] Thompson MT, Berg MC, Tobias IS, Lichter JA, Rubner MF, Van Vliet KJ. Biochemical functionalization of polymeric cell substrata can alter mechanical compliance. Biomacromolecules 2006;7(6):1990–5.
[269] Lee M, Kang DK, Yang HK, Park KH, Choe SY, Kang C, et al. Protein nanoarray on Prolinker™ surface constructed by atomic force microscopy dip-pen nanolithography for analysis of protein interaction. Proteomics 2006;6(4):1094–103.
[270] Sahin O, Erina N. High-resolution and large dynamic range nanomechanical mapping in tapping-mode atomic force microscopy. Nanotechnology 2008;19(44):445717.
[271] Ankam S, Suryana M, Chan LY, Moe AA, Teo BK, Law JB, et al. Substrate topography and size determine the fate of human embryonic stem cells to neuronal or glial lineage. Acta Biomater 2013;9(1):4535–45.
[272] Tan KK, Tann JY, Sathe SR, Goh SH, Ma D, Goh EL, et al. Enhanced differentiation of neural progenitor cells into neurons of the mesencephalic dopaminergic subtype on topographical patterns. Biomaterials 2015;43:32–43.
[273] Unadkat HV, Hulsman M, Cornelissen K, Papenburg BJ, Truckenmuller RK, Carpenter AE, et al. An algorithm-based topographical biomaterials library to instruct cell fate. Proc Natl Acad Sci USA 2011;108(40):16565–70.
[274] Gu Y, Zhu J, Xue C, Li Z, Ding F, Yang Y, et al. Chitosan/silk fibroin-based, Schwann cell-derived extracellular matrix-modified scaffolds for bridging rat sciatic nerve gaps. Biomaterials 2014;35(7):2253–63.
[275] Liu X, Zhang F, Wang Q, Gao J, Meng J, Wang S, et al. Platelet-inspired multiscaled cytophilic interfaces with high specificity and efficiency toward point-of-care cancer diagnosis. Small 2014;10(22):4677–83.
[276] Zhao L, Mei S, Chu P, Zhang Y, Wu Z. The influence of hierarchical hybrid micro/nano-textured titanium surface with titania nanotubes on osteoblast functions. Biomaterials 2010;31(19):5072–82.
[277] Kubo K, Tsukimura N, Iwasa F, Ueno T, Saruwatari L, Aita H, et al. Cellular behavior on TiO_2 nanonodular structures in a micro-to-nanoscale hierarchy model. Biomaterials 2009;30(29):5319–29.
[278] Gittens R, McLachlan T, Olivares-Navarrete R, Cai Y, Berner S, Tannenbaum R, et al. The effects of combined micron-/submicron-scale surface roughness and nanoscale features on cell proliferation and differentiation. Biomaterials 2011;32(13):3395–403.
[279] Tsukimura N, Yamada M, Iwasa F, Minamikawa H, Att W, Ueno T, et al. Synergistic effects of UV photofunctionalization and micro-nano hybrid topography on the biological properties of titanium. Biomaterials 2011;32(19):4358–68.

[280] Tocce EJ, Smirnov VK, Kibalov DS, Liliensiek SJ, Murphy CJ, Nealey PF. The ability of corneal epithelial cells to recognize high aspect ratio nanostructures. Biomaterials 2010;31(14):4064–72.

[281] Jia Z, Xiu P, Li M, Xu X, Shi Y, Cheng Y, et al. Bioinspired anchoring AgNPs onto micro-nanoporous TiO_2 orthopedic coatings: trap-killing of bacteria, surface-regulated osteoblast functions and host responses. Biomaterials 2016;75:203–22.

[282] Moffa M, Sciancalepore AG, Passione LG, Pisignano D. Combined nano- and micro-scale topographic cues for engineered vascular constructs by electrospinning and imprinted micro-patterns. Small 2014;10(12):2439–50.

[283] López-Bosque MJ, Tejeda-Montes E, Cazorla M, Linacero J, Atienza Y, Smith KH, et al. Fabrication of hierarchical micro-nanotopographies for cell attachment studies. Nanotechnology 2013;24(25):255305.

[284] Kim J, Bae WG, Choung HW, Lim KT, Seonwoo H, Jeong HE, et al. Multiscale patterned transplantable stem cell patches for bone tissue regeneration. Biomaterials 2014;35(33):9058–67.

[285] Yang K, Jung H, Lee HR, Lee JS, Kim SR, Song KY, et al. Multiscale, hierarchically patterned topography for directing human neural stem cells into functional neurons. ACS Nano 2014;8(8):7809–22.

[286] Bao L, Cheng X, Huang X, Guo L, Pang S, Yee A. Nanoimprinting over topography and multilayer three-dimensional printing. J Vac Sci Technol B 2002;20(6):2881–6.

[287] Eliason MT, Charest JL, Simmons BA, García AJ, King WP. Nanoimprint fabrication of polymer cell substrates with combined microscale and nanoscale topography. J Vac Sci Technol B 2007;25(4):L31–4.

[288] Cukierman E, Pankov R, Stevens DR, Yamada KM. Taking cell-matrix adhesions to the third dimension. Science 2001;294(5547):1708–12.

[289] Bryant SJ, Chowdhury TT, Lee DA, Bader DL, Anseth KS. Crosslinking density influences chondrocyte metabolism in dynamically loaded photocrosslinked poly(ethylene glycol) hydrogels. Ann Biomed Eng 2004;32(3):407–17.

[290] Park Y, Lutolf MP, Hubbell JA, Hunziker EB, Wong M. Bovine primary chondrocyte culture in synthetic matrix metalloproteinase-sensitive poly(ethylene glycol)-based hydrogels as a scaffold for cartilage repair. Tissue Eng 2004;10(3–4):515–22.

[291] Fouchard J, Bimbard C, Bufi N, Durand-Smet P, Proag A, Richert A, et al. Three-dimensional cell body shape dictates the onset of traction force generation and growth of focal adhesions. Proc Natl Acad Sci USA 2014;111(36):13075–80.

[292] Hogrebe NJ, Gooch KJ. Direct influence of culture dimensionality on human mesenchymal stem cell differentiation at various matrix stiffnesses using a fibrous self-assembling peptide hydrogel. J Biomed Mater Res A 2016;104(9):2356–68.

[293] Fischbach C, Chen R, Matsumoto T, Schmelzle T, Brugge JS, Polverini PJ, et al. Engineering tumors with 3D scaffolds. Nat Methods 2007;4(10):855–60.

[194] Aljitawi OS, Li D, Xiao Y, Zhang D, Ramachandran K, Stehno-Bittel L, et al. A novel three-dimensional stromal-based model for *in vitro* chemotherapy sensitivity testing of leukemia cells. Leuk Lymphoma 2014;55(2):378–91.

[295] Talukdar S, Kundu SC. A non-mulberry silk fibroin protein based 3D *in vitro* tumor model for evaluation of anticancer drug activity. Adv Funct Mater 2012;22(22):4778–88.

[296] Bruce A, Evans R, Mezan R, Shi L, Moses BS, Martin KH, et al. Three-dimensional microfluidic tri-culture model of the bone marrow microenvironment for study of acute lymphoblastic leukemia. PLoS One 2015;10(10):e0140506. Erratum in: PLoS One 2015;10(12):e0146203.

[297] Lutolf MP, Hubbell JA. Synthetic biomaterials as instructive extracellular microenvironments for morphogenesis in tissue engineering. Nat Biotechnol 2005;23(1):47–55.

[298] Sun Y, Jallerat Q, Szymanski JM, Feinberg AW. Conformal nanopatterning of extracellular matrix proteins onto topographically complex surfaces. Nat Methods 2015;12(2):134–6.

[299] Perschmann N, Hellmann JK, Frischknecht F, Spatz JP. Induction of malaria parasite migration by synthetically tunable microenvironments. Nano Lett 2011;11(10):4468–74.

[300] Aydin D, Louban I, Perschmann N, Blümmel J, Lohmüller T, Cavalcanti-Adam EA, et al. Polymeric substrates with tunable elasticity and nanoscopically controlled biomolecule presentation. Langmuir 2010;26(19):15472–80.

[301] Li S, Wang X, Cao B, Ye K, Li Z, Ding J. Effects of nanoscale spatial arrangement of arginine-glycine-aspartate peptides on dedifferentiation of chondrocytes. Nano Lett 2015;15(11):7755–65.

[302] Kruss S, Erpenbeck L, Schön MP, Spatz JP. Circular, nanostructured and biofunctionalized hydrogel microchannels for dynamic cell adhesion studies. Lab Chip 2012;12(18):3285–9.

[303] Chaudhuri O, Koshy ST, Branco da Cunha C, Shin JW, Verbeke CS, Allison KH, et al. Extracellular matrix stiffness and composition jointly regulate the induction of malignant phenotypes in mammary epithelium. Nat Mater 2014;13(10):970–8.

[304] Madl CM, Katz LM, Heilshorn SC. Bio-orthogonally crosslinked, engineered protein hydrogels with tunable mechanics and biochemistry for cell encapsulation. Adv Funct Mater 2016;26(21):3612–20.

[305] White ES. Lung extracellular matrix and fibroblast function. Ann Am Thorac Soc 2015;12(Suppl 1):S30–3.

[306] Kisseleva T, Brenner DA. Mechanisms of fibrogenesis. Exp Biol Med 2008;233(2):109–22.

[307] Burdick JA, Murphy WL. Moving from static to dynamic complexity in hydrogel design. Nat Commun 2012;3:1269.

[308] Tibbitt MW, Anseth KS. Dynamic microenvironments: the fourth dimension. Sci Transl Med 2012;4(160):160ps24.

[309] Guvendiren M, Burdick JA. Stiffening hydrogels to probe short- and long-term cellular responses to dynamic mechanics. Nat Commun 2012;3:792.

[310] Young JL, Engler AJ. Hydrogels with time-dependent material properties enhance cardiomyocyte differentiation *in vitro*. Biomaterials 2011;32(4):1002–9.

[311] Khetan S, Guvendiren M, Legant WR, Cohen DM, Chen CS, Burdick JA. Degradation-mediated cellular traction directs stem cell fate in covalently crosslinked three-dimensional hydrogels. Nat Mater 2013;12(5):458–65.

[312] Le DM, Kulangara K, Adler AF, Leong KW, Ashby VS. Dynamic topographical control of mesenchymal stem cells by culture on responsive poly(ε-caprolactone) surfaces. Adv Mater 2011;23(29):3278–83.

[313] Kloxin AM, Kasko AM, Salinas CN, Anseth KS. Photodegradable hydrogels for dynamic tuning of physical and chemical properties. Science 2009;324(5923):59–63.